A COMPARISON BETWEEN THEORETICAL AND EXPERI[illegible]TURAL MODES AND FREQUENCIES OF A BUILT-UP DEL[illegible]EN

A Thes[illegible]

Presented to

the Faculty of the Department of Engineering

University of Virginia

In Partial Fulfillment

of the Requirements for the Degree

Master of Aeronautical Engineering

---

by

Paul Waner, Jr.

July 1955

A COMPARISON BETWEEN THEORETICAL AND EXPERIMENTAL NATURAL MODES AND FREQUENCIES OF A BUILT-UP DELTA WING SPECIMEN

A Thesis

Presented to

the Faculty of the Department of Engineering

University of Virginia

In Partial Fulfillment

of the Requirements for the Degree

Master of Aeronautical Engineering

---

by

Paul Waner, Jr.

July 1955

APPROVAL SHEET

This thesis is submitted in partial fulfillment of
the requirements for the degree of
Master of Aeronautical Engineering

Paul Wanen, Jr.
Author

Approved:

John M. Hedgeth
Faculty Advisor

For Subcommittee

Chairman, Committee on Graduate Studies
in Engineering

July 1955

ACKNOWLEDGMENT

The author is grateful to Mr. John M. Hedgepeth and Mr. Edwin T. Kruszewski who checked the work and gave many helpful suggestions, and to the National Advisory Committee for Aeronautics for their permission to present this work which was carried out under their auspices at the Langley Aeronautical Laboratory.

TABLE OF CONTENTS

LIST OF TABLES

LIST OF FIGURES

SYMBOLS

A	stiffness matrix
E	Young's modulus of elasticity
I	moment of inertia
M	mass matrix
P	matrix of the loads
P_m	concentrated lateral load at station m
$c(y)$	wing chord (see Figure 4)
m	mass
m_{11}, m_{12}, m_{22}	parameters defined by equation (30)
$p(x,y)$	lateral load at station (x,y)
$p_n(y)$	generalized load defined by equation (10)
r	matrix defined by equation (19)
t	thickness of cover sheet
w	deflection of free structure
x	chordwise coordinate
y	spanwise coordinate
z	height of middle plane of cover sheet above neutral surface of wing
Δ	influence coefficient matrix
α_{11}, α_{12}, α_{22}	parameters defined by equation (31)
δ_{mn}	Kronecker delta
ϵ	distance between spanwise stations

η deflection of fixed structure

μ Poisson's ratio

Φ_n function of y, coefficient in power series for deflection

$$\eta = \sum_{n=0}^{3} x^n \Phi_n(y)$$

Ψ_n function of y, coefficient in power series for deflection

$$w = \sum_{n=0}^{3} x^n \Psi_n(y)$$

ω natural frequency

Subscripts:

a antisymmetric

s symmetric

Superscripts:

$\sim$ spar

$\cdot$ rib

$-$ cover sheet

$\wedge$ stringer

$*$ spar and cover sheet and stringer

$\cdot\cdot$ rib and concentrated weights

Matrix notation:

$[\ ]$	rectangular or square matrix
$\lfloor\ \rfloor$	row matrix
$\vert\ \vert$	column matrix
$\begin{bmatrix} \diagdown \end{bmatrix}$	diagonal matrix

CHAPTER I

INTRODUCTION

Many present day aircraft and guided missiles are equipped with low-aspect-ratio wings of a delta plan form. Since all of these aircraft and missiles have high performance characteristics, a flutter analysis is usually necessary. However, the flutter analysis depends to a great extent on the accuracy of the free-free natural modes and frequencies of the wing. These natural modes and frequencies can also be useful in other dynamic problems, such as landing impact and gust loads. In the past, when airplane wings usually had high aspect ratios, the natural modes and frequencies could, in general, be found by methods using simple beam theory. For airplanes with low-aspect-ratio wings, the vibration problem is complicated by chordwise bending of the wing which must be taken into account. The methods using beam theory do not account for this chordwise bending; thus, for a delta wing or any low-aspect-ratio wing, recourse must be made to more elaborate methods to determine the natural modes and frequencies.

In the vibration problem, one of the first methods that presents itself is the direct solution of the partial-differential equations of equilibrium of the structure. However, even for a thin isotropic plate, the direct solution

of the differential equation is extremely complicated and solutions for only a few isolated boundary conditions have been obtained. (See, for example, ref. 5.) For a built-up wing the differential equation approach would present insurmountable difficulties. Another method widely used in vibration analysis is based on the Rayleigh-Ritz principle. This principle says that the maximum strain energy minus the maximum kinetic energy of the wing must be an extremum. To apply this principle to a specific structure, the first step is to express the strain and kinetic energy of the structure in terms of the deflection. The deflection is then represented by a series expansion of functions with unknown coefficients; the strain energy minus the kinetic energy is differentiated with respect to each of the unknown coefficients of the series and the result set equal to zero. In general, it is necessary to use a finite series. If the series has n terms then there will be a set of n equations from which the n unknown coefficients and the frequency can be found. The application of the Rayleigh-Ritz method to a constant thickness rectangular plate is presented by Timoshenko in reference 8 and also by D. Young in reference 12. The Rayleigh-Ritz method has a disadvantage in that the coefficients of the set of equations are

integrals which consist of the functions which were used in the series expansion. The labor involved in evaluating these integrals becomes excessive when very many terms are used in the series.

A method which shows considerable promise for the vibration analysis of complicated structures is the influence coefficient approach. An advantage that this method has over the other two methods is that the complicated vibration problem is divided into several simpler parts: (1) the determination of the deflections of the structure in terms of the static loads placed on it, (2) the determination of the maximum dynamic loads acting on the structure, and (3) the substitution of the dynamic loads for the static loads. Another advantage of this method is that the influence coefficients can be used for other purposes, such as static aeroelastic problems.

The determination of the natural modes and frequencies by the influence coefficient approach requires that the influence coefficients be known. For thin solid wings of low aspect ratio, static deflection analyses have been made by using the well known plate theory. A direct attack on the partial-differential equation of a constant thickness plate by using the separation of variables procedure is given in reference 11. A method which allows for a gradually varying thickness and chord is presented in reference 2.

In reference 2, the deflection of the wing was represented by a power series in the chordwise direction with the coefficients of the power series as functions of the spanwise direction. The first term of the power series represents the transverse displacement, the second term represents the twist, the third term represents a parabolic curvature in the chordwise direction, and so forth. In reference 2, only the first two terms of the power series were used. An expression was then written for the total potential energy of the structure; the total potential energy being defined as the strain energy of bending minus the potential energy of the lateral loads. The expression for the deflection was then substituted into the total potential energy and the calculus of variations used to minimize the total potential energy with respect to the coefficients of the power series. When this was done, there resulted two ordinary differential equations which could be solved to give the deflection in terms of the loads. A method for determining the deflections of plates by starting with the partial-differential equations of plate theory and applying the Galerkin procedure was presented by Schuerch in reference 3. Since Schuerch expressed the deflection of the wing by the same power series of two terms as used in reference 2, his results were very similar to those found in that reference.

An extension of reference 2 to include parabolic chordwise deflections is given in reference 6. The method of analysis of reference 6 is identical to that used in reference 2. That is, the total potential energy of the plate with lateral loads was written, the power-series shape substituted into it and it was then minimized with respect to the coefficients of the power series. In this case, three ordinary differential equations resulted. Experimental results for the deflections of several triangular plates of different shapes under uniform static loads are included in this paper. When the theoretical deflections using two and three terms are compared with the experimental deflections it is seen that there is good agreement, with, of course, better agreement for the three term solution.

The methods mentioned above are applicable to thin low-aspect-ratio solid wings. If a built-up wing is very thin and has closely spaced spars and ribs and a thick cover sheet, then its influence coefficients can be found by considering it as a solid wing and then using plate theory. If the built-up wing does not have closely spaced spars and ribs, then serious errors can result if plate theory is used. For these cases, it is necessary to use methods which account for the spars and ribs as separate entities instead of

considering their stiffness as simply adding to the cover stiffness. Several such methods have appeared in the literature and are listed below.

(1) Schuerch's method (ref. 4): Schuerch has developed a "wide beam theory" based on simple beam equations but which gives an approximate expression for the deflections of low-aspect-ratio wings. His method was to idealize the structure into a group of alternating simple beams and torsion tubes running in the spanwise direction. The beams represent the normal load carrying ability of the spars and cover. The torsion tubes represent the shear carrying capacity of the cover. Since the wing is only allowed a translation and rotation, the flexibility of the ribs is neglected.

(2) Levy's method (ref. 1): Levy's method is one of consistent deformations; that is, the loads in terms of the deflections for each individual wing component are found. The resulting loads are then added together so that the loads at all the points on the wing are found in terms of all the deflections. The wing components that are considered are: (a) the spars and cover sheet in spanwise bending, (b) the ribs and part of the cover sheet in chordwise bending, and (c) the cover sheet in torsion.

(3) William's method (ref. 10): William's has outlined a method which uses the partial-differential equations of plate theory. However, instead of directly solving the partial-differential equations he replaces the derivatives with finite differences. This results in a large order simultaneous set of equations which can be solved by conventional methods. The disadvantage of William's method is that it is applicable only to wings which have closely spaced spars and ribs and a thick cover sheet.

(4) Stein-Sanders method (ref. 7): The Stein-Sanders method is essentially an extension of the method presented in references 2 and 6. In this method, the spars and ribs are considered as separate entities. Three terms of the power series are again used to represent the deflection of the wing, but the total potential energy to be minimized now includes the strain energy of the spars and ribs. In order to simplify the calculations and make the procedure readily applicable to any wing, difference-equation methods are used in the process of expressing and minimizing the potential energy. Thus, there is yielded a system of simultaneous algebraic equations which relate the deflections to the lateral loads.

The coefficients which relate the deflections to the lateral loads are called the stiffness coefficients and the matrix of the stiffness coefficients is called the stiffness matrix. The influence coefficient matrix is obtained by inverting the stiffness matrix.

In the present paper, a comparison will be made between the experimental and theoretical natural modes and frequencies of vibration of a built-up delta wing. The theoretical calculations will employ the influence coefficient approach where the influence coefficients are obtained from the method presented by Stein and Sanders (ref. 7). As has been mentioned previously, the Stein-Sanders method treats the cover sheets, spars, and ribs as separate entities. The strain energy expression of these terms and also a general outline of the Stein-Sanders method is given in Appendix A.

CHAPTER II

DESCRIPTION OF BUILT-UP DELTA WING SPECIMEN

The built-up delta wing specimen to be analyzed is considered representative of the load carrying structure of a real delta wing. The center section of the wing, where the fuselage would fit, is of constant thickness. Outboard of this center section there is a constant spanwise taper; the chordwise sections are of constant thickness. The internal structure consists of spars and ribs. (See Figure 1.) There are five spars which are perpendicular to the center line of the wing and one spar which is inclined at a 45° angle to the center line. Spars 1, 2, and 3 have an I type cross section; spars 4, 5, and 6 are channel shaped. The ribs are located at 8-inch intervals and are parallel to the center line of the wing. All of the ribs are channel shaped. It should be noted that in Figure 1, rib No. 2 is shown as only one rib; however, in the actual wing, two ribs which were very close together were located there. Several other small changes have been made in drawing the idealized structure shown in Figure 1, but these changes should not effect the accuracy by which this idealized structure represents the actual structure.

The internal structure of the wing was covered by a constant thickness sheet of aluminum which was riveted to the

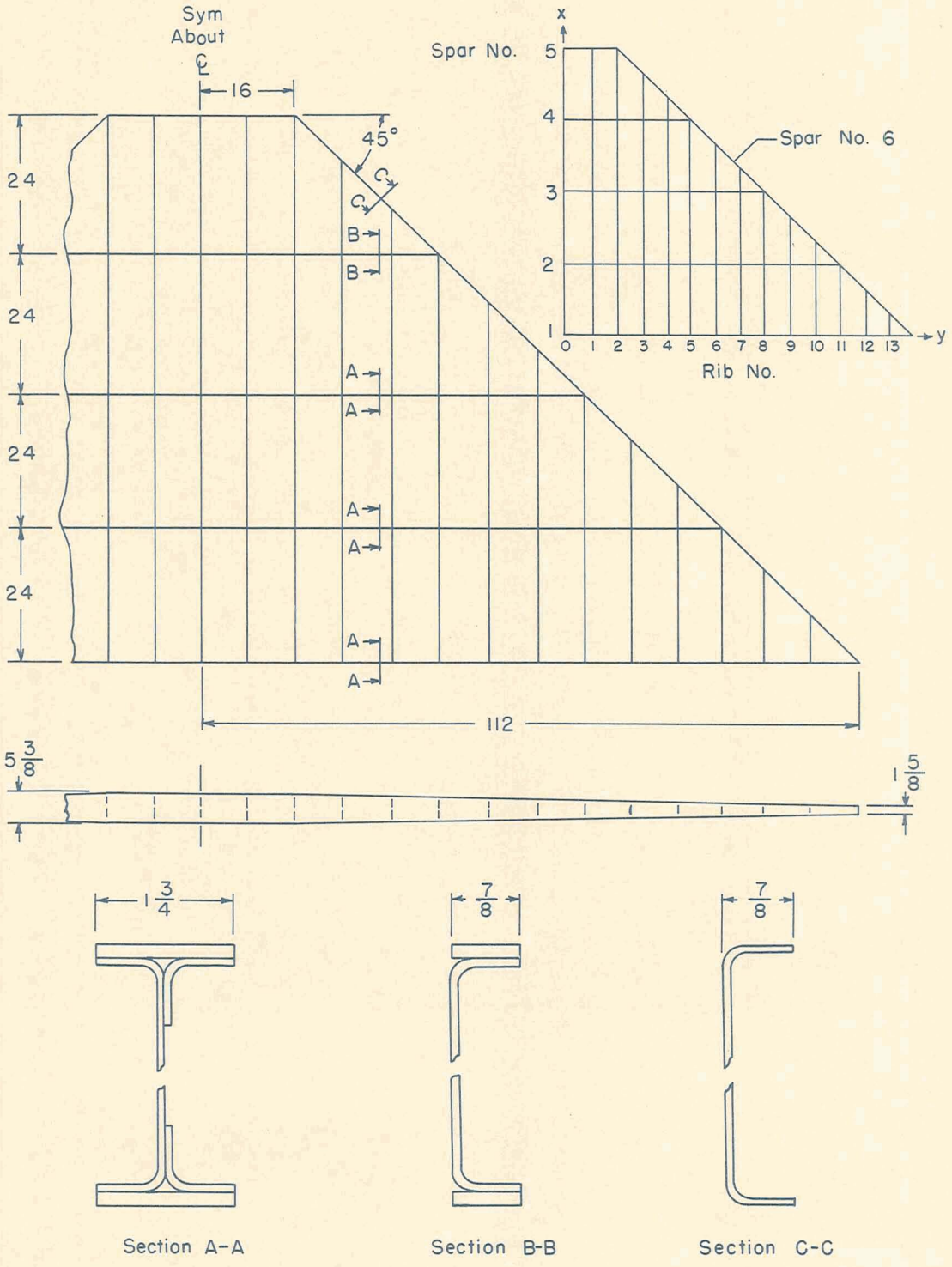

FIGURE 1

INTERNAL STRUCTURE OF WING

spars and ribs. There are a total of 16 stringers which were riveted to the outside of the cover. The location of these stringers is shown in Figure 2.

A brief discussion of the physical properties and the stiffness and mass properties of the wing components is given below.

(1) Physical properties: The wing is constructed entirely of 24ST aluminum alloy. The physical properties of 24ST that will be needed in this paper are shown below. (See ref. 13.)

Young's modulus of elasticity, $lb/in.^2$ . .	10.6×10^6
Weight, $lb/in.^3$	0.100
Poisson's ratio	1/3

(2) Spars: The weight of the spars was found by using actual measured dimensions and dimensions which were slightly changed from the original specifications. In this way, a calculated spar weight was obtained which was equal to the measured spar weight. By using these dimensions, the weight per inch and moment of inertia of the spars at 8-inch intervals along the span were calculated and are tabulated in Table I. The weight listed is the weight per inch of a cross section normal to the y-axis and includes the weight of the heads of the rivets which were used to fasten the cover to the spars. The rivet-head weight was

Stringer No.	x coordinate
16	91.31
15	86.44
14	81.56
13	76.69
12	66.75
11	62.25
10	57.75
9	53.25
8	42.75
7	38.25
6	33.75
5	29.25
4	18.75
3	14.25
2	9.75
1	5.25

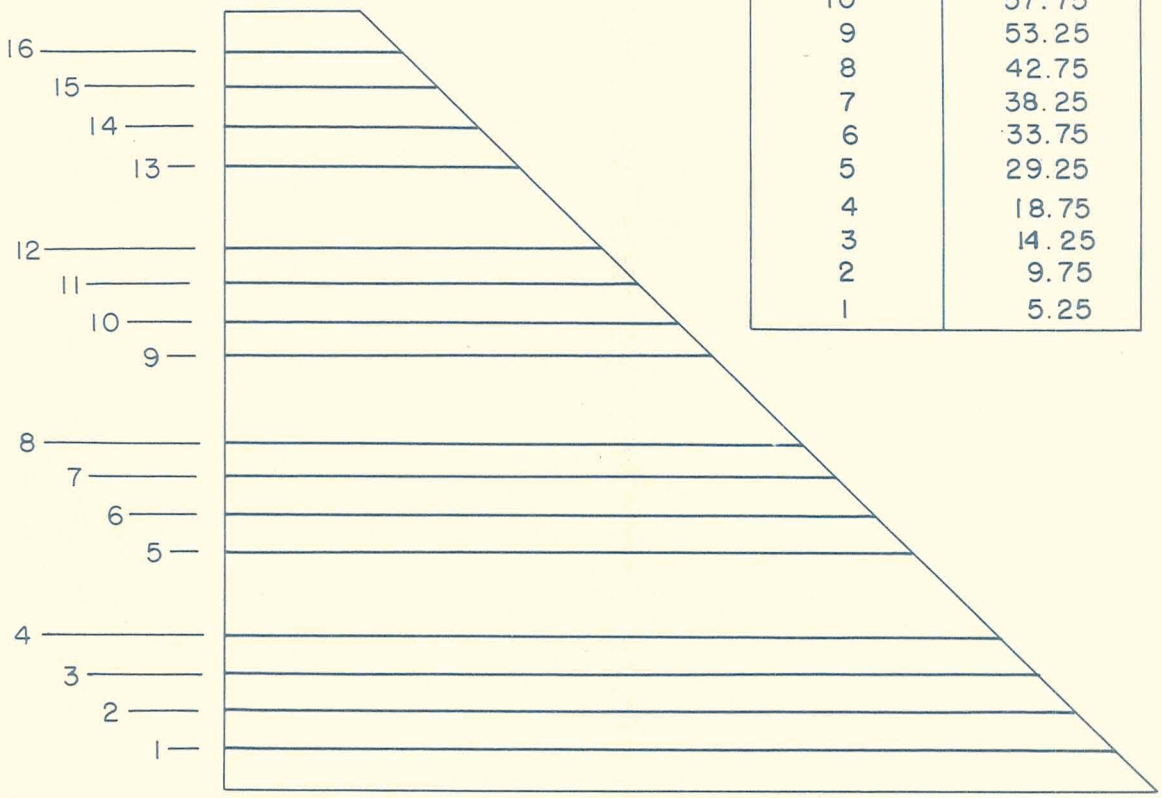

FIGURE 2

STRINGER LOCATION

TABLE I

SPAR WEIGHT AND MOMENT OF INERTIA

Station y in.	Spar No. 1		Spar No. 2		Spar No. 3		Spar No. 4		Spar No. 5		Spar No. 6	
	$\tilde{w}_{1y}$ lb/in.	$\tilde{I}_{1y}$ $in.^4$	$\tilde{w}_{2y}$ lb/in.	$\tilde{I}_{2y}$ $in.^4$	$\tilde{w}_{3y}$ lb/in.	$\tilde{I}_{3y}$ $in.^4$	$\tilde{w}_{4y}$ lb/in.	$\tilde{I}_{4y}$ $in.^4$	$\tilde{w}_{5y}$ lb/in.	$\tilde{I}_{5y}$ $in.^4$	$\tilde{w}_{6y}$ lb/in.	$\tilde{I}_{6y}$ $in.^4$
0	0.15715	7.7880	0.14550	6.8764	0.17323	8.9730	0.08469	3.6300	0.05936	2.3006		
8	.15715	7.7880	.14550	6.8764	.17323	8.9730	.08469	3.6300	.05936	2.3006		
16	.15715	7.7880	.14550	6.8764	.17323	8.9730	.08469	3.6300	.05936	2.3006	0.08395	2.3006
24	.15498	6.8180	.14331	6.0047	.17099	7.8705	.08244	3.1572			.08083	1.9960
32	.15281	5.9173	.14113	5.1969	.16876	6.8453	.08020	2.7223			.07772	1.7180
40	.15065	5.0850	.13894	4.4520	.16652	5.8964	.07795	2.3242			.07460	1.4654
48	.14848	4.3199	.13676	3.7687	.16428	5.0225					.07149	1.2371
56	.14632	3.6210	.13457	3.1462	.16204	4.2223					.06838	1.0321
64	.14414	2.9872	.13239	2.5832	.15980	3.4961					.06526	.8494
72	.14198	2.4175	.13020	2.0789							.06215	.6878
80	.13981	1.9108	.12801	1.6319							.05904	.5462
88	.10581	1.1379	.12583	1.2414							.05592	.4237
96	.07182	.5955									.05281	.3191
104	.06965	.4159									.04970	.2313
112	.06748	.2697									.04657	.1594

determined by accurately approximating the number of rivets and then multiplying by the weight of the heads of one rivet. The moment of inertia listed in Table I is for a cross section normal to the spar.

(3) Ribs: The weight and moment of inertia of the ribs are given in Table II. The weight listed is the weight of each rib and includes the weight of the cover-rib rivet heads.

(4) Cover sheet: The nominal cover sheet thickness specified was 0.072 inch, but the measured average thickness of the cover was found to be 0.0696 inch. A dimension which will be useful in later calculations is the height of the middle plane of the cover above the neutral surface of the wing. This height which is called z is tabulated in Table III.

(5) Stringers: The stringers are $3/4 \times 3/4 \times 1/8$ inch standard angles. The measured cross sectional area of the stringers was found to be 0.1689 square inch. This area was obtained by first weighing all the stringers and then dividing this weight by the product of the stringer length and density. The weight of one stringer was then found by multiplying the measured area by the density and adding the weight

TABLE II

RIB WEIGHT AND MOMENT OF INERTIA

Rib No.	$\dot{w}$ lb	$\dot{I}$ $in.^4$
0	3.3690	1.0604
1	3.3690	1.0604
2	9.7126	3.0694
3	2.9136	.9064
4	2.4650	.7677
5	2.0867	.6435
6	1.7821	.5331
7	1.4446	.4356
8	1.1811	.3504
9	.9026	.2767
10	.6691	.2136
11	.4706	.1604
12	.2820	.1164
13	.1135	.0807

TABLE III

COVER SHEET HEIGHT

Station y in.	Cover height z_y in.
0	2.7152
8	2.7152
16	2.7152
24	2.5593
32	2.4033
40	2.2474
48	2.0915
56	1.9356
64	1.7797
72	1.6238
80	1.4678
88	1.3119
96	1.1560
104	1.0001
112	.8442

of the cover-stringer rivet heads; this weight was 0.01920 lb/in. The moment of inertia of one stringer, $\hat{I}$, about the neutral surface of the wing and the number of stringers on the top and bottom cover at 8 inch spanwise intervals are listed in Table IV.

(6) Reinforcements and spar to rib rivets: In the construction of the delta wing, several small reinforcements were added at critical points, and their weight should be taken into account. Also, the rivet-head weight of the rivets used to connect the spars to the ribs should be included in the weight analysis. The location and weight of the reinforcements and the spar-to-rib rivets are tabulated in Table V.

Table VI is included to show the total calculated weight of the various components and their percentage weight of the total calculated weight. By adding up the weight of the components, the total calculated weight was found to be about 408.6 pounds. It is interesting to note that the rivet-head weight was about 5 per cent of the total weight. A total measured weight of 409 pounds was obtained by weighing the wing after it was completely assembled.

TABLE IV

STRINGER MOMENT OF INERTIA

Station y in.	$\hat{I}_y$ $in.^4$	$\hat{N}_y$
0	1.4969	32
8	1.4969	32
16	1.4969	32
24	1.3442	30
32	1.1997	26
40	1.0635	24
48	.9354	22
56	.8156	18
64	.7039	16
72	.6005	14
80	.5053	10
88	.4183	8
96	.3395	6
104	.2689	2
112	0	0

TABLE V

WEIGHT OF REINFORCEMENTS AND SPAR TO RIB RIVETS

Station y in.	Chordwise location				
	x = 0 $w^{(r)}(0,y)$ lb	x = 24 $w^{(r)}(24,y)$ lb	x = 48 $w^{(r)}(48,y)$ lb	x = 72 $w^{(r)}(72,y)$ lb	x = 96 $w^{(r)}(96,y)$ lb
0	0.02634	0.02634	0.02634	0.00993	0.48893
8	.02634	.02634	.02634	.00993	.00993
16	.05814	.05814	.05814	.01986	.28836
24	.02470	.02470	.02470	.00993	
32	.02163	.02163	.02163	.00851	
40	.01999	.01999	.01999	.00851	
48	.01693	.01693	.01693		
56	.01387	.01387	.01387		
64	.01223	.01223	.00567		
72	.00918	.00918			
80	.00754	.00754			
88	.00284	.00284			
96	.00284				
104	.00284				
112	0				

TABLE VI

CALCULATED WEIGHT OF WING COMPONENTS

Item	Weight lb	Per cent of total
Spars	87.181	21.34
Ribs	58.154	14.23
Cover sheet	180.287	44.12
Stringers	80.313	19.66
Reinforcements	1.748	.43
Spar to rib rivets	.900	.22
Total weight	408.583	100.00

CHAPTER III

DESCRIPTION OF TEST SET UP

The experimental determination of the natural free-free modes and frequencies of the built-up delta wing was carried out by Mr. Eldon E. Kordes in the Structures Research Laboratory of the NACA. To obtain the free-free condition, the wing was supported by two wires which were connected to an overhead scaffold. A picture of the wing in its free-free condition is shown in Figure 3. The wing was vibrated by four symmetrically placed shakers connected to the wing. These shakers could apply a maximum force of 50 pounds and had a maximum travel of 1 inch; their frequency range was from 2-1/2 to 500 cycles per second. The shakers were part of the MB Manufacturing Co. C-1-S exciter system. This system allowed control of the force applied by each shaker. The control panel of the exciter system is shown on the left side of Figure 3.

The phase relation between different points on the wing and the amplitude of the points during a vibration test was obtained by mounting MB Type 124 self-generating velocity pickups on the wing. These pickups are shown in Figure 3. The "pickups" on the left side of the wing with no lead-in wires attached to them are weights which were used to balance the weight of the pickups on the right side. However, two

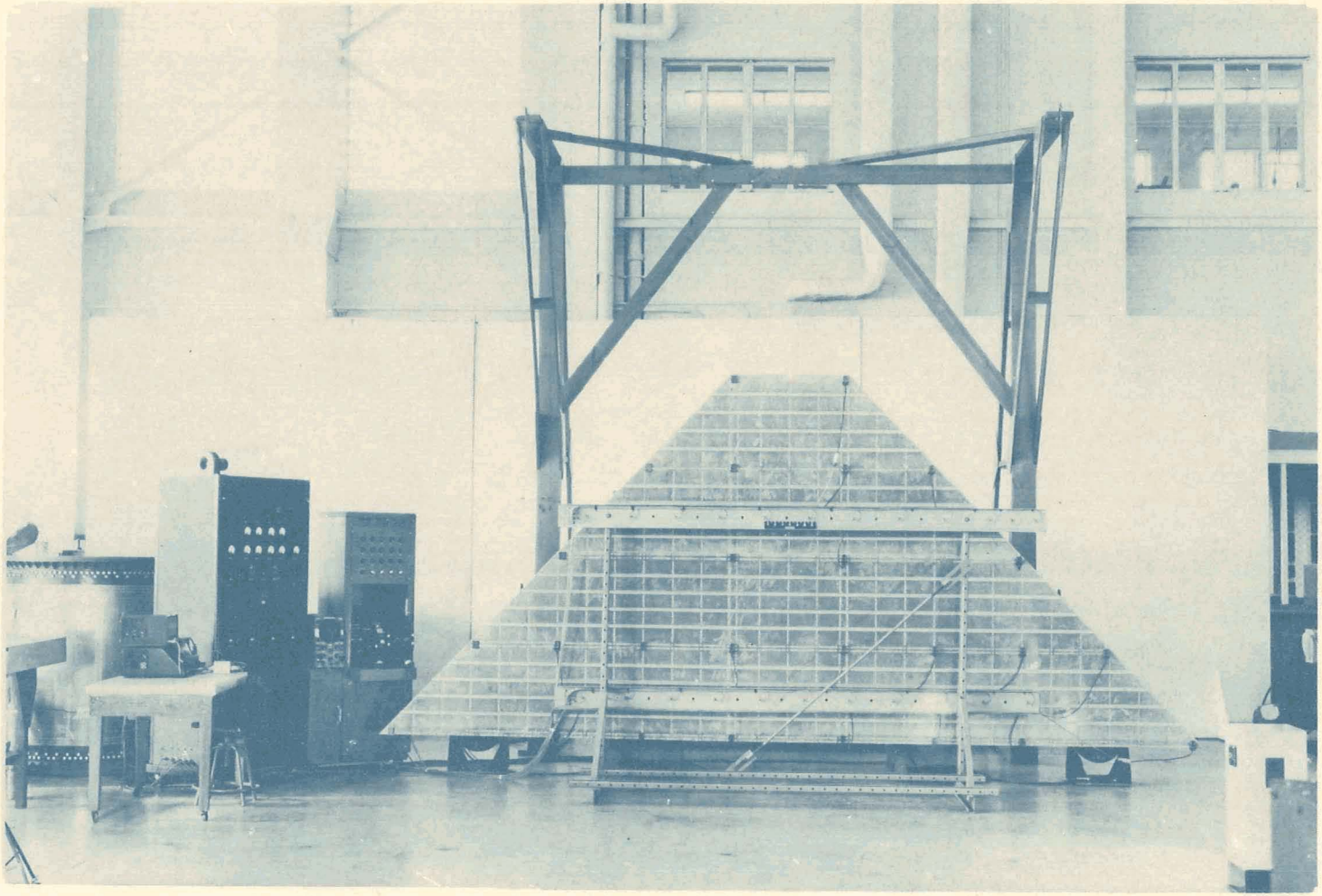

L-88268

FIGURE 3

VIBRATION TEST SETUP FOR DELTA WING SPECIMEN

pickups were located on the left side to provide a check on the symmetry of the modes. The output voltage from the pickups was fed into an oscillograph. The control panel used to select the pickup voltage is the small cabinet in Figure 3. The natural frequencies of the wing were determined by varying the frequency of the shakers until the trace of the pickup voltage on the oscillograph reached a maximum amplitude. The voltage from a pickup attached to a shaker was fed into a C. G. Conn model GT-2 Stroboconn from which the frequency in cycles per second was determined. The node lines were found by moving a portable pickup over the wing until the oscillograph showed that the amplitude was zero.

The natural frequencies of the wing were found with the shakers and pickups attached; therefore, it is necessary to include their weight in with the wing weight to be used in the vibration analysis. Each shaker attachment weighed 2 pounds and each pickup weighed 0.7 pound. The total weight of these accessories is shown below.

4 Shaker attachments, lb	8.0
26 Pickups, lb	18.2
Total accessory weight, lb	26.2

The total weight of the wing during a vibration test is shown below.

	Measured	Calculated
Total weight, lb	409	408.583
Accessory weight, lb	26.2	26.2
Total weight during a vibration test, lb	435.2	434.783

Since it is important to know the distribution of the shaker attachments and pickups in the theoretical analysis, the location and weight of the shaker attachments and pickups are given in Table VII.

TABLE VII

SHAKER ATTACHMENT AND PICKUP WEIGHT

Station y in.	Chordwise location				
	x = 0 $w^{(t)}_{(0,y)}$ lb	x = 24 $w^{(t)}_{(24,y)}$ lb	x = 48 $w^{(t)}_{(48,y)}$ lb	x = 72 $w^{(t)}_{(72,y)}$ lb	x = 96 $w^{(t)}_{(96,y)}$ lb
16	.70	.70	.70	.70	.70
40	.70	.70	2.00	.70	
64	.70	.70	.70		
88	2.00	.70			
112	.70				

CHAPTER IV

DISCUSSION OF INFLUENCE COEFFICIENT APPROACH

Since the theoretical natural modes and frequencies of the delta wing are to be found by the influence coefficient approach, it is felt worthwhile to consider this method in detail for a simple example problem. The example problem to be treated is that of determining the natural modes and frequencies of symmetric vibration of a free-free beam with variable stiffness properties. A sketch of the beam in a symmetrically deflected position is shown below. In this sketch η is the distance of any point on the beam above the center line point and w is the actual deflection of the beam above its position at rest.

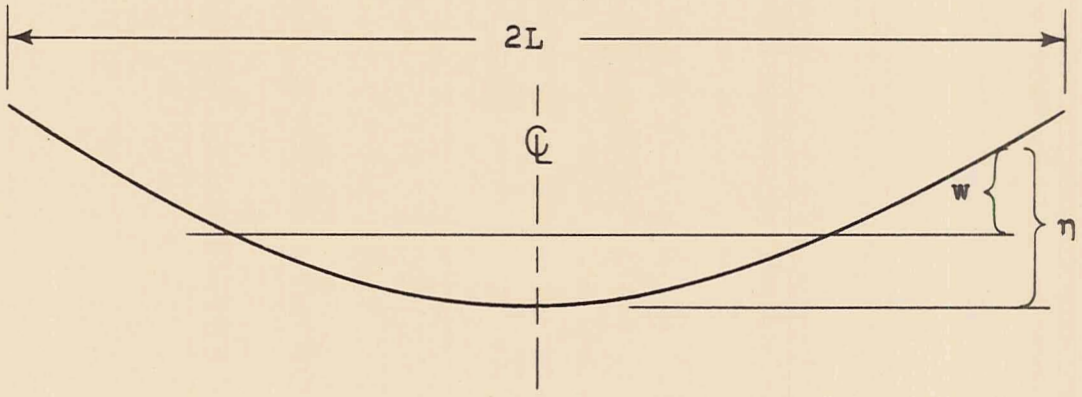

When the natural modes and frequencies are to be found by the influence coefficient approach, the first thing needed is the influence coefficients. However, for a

free-free beam, the influence coefficients can not be found directly. What can be done however, is first to find the influence coefficients for the beam in some fixed condition. Then by releasing the beam and by considering the appropriate dynamic equilibrium conditions, these "fixed" influence coefficients can be used to find the free-free natural modes and frequencies. For this analysis, the "fixed" influence coefficients will be found by considering the beam to be simply supported at the center line and acted on by symmetric loads. The beam, simply supported at the center line, with two symmetric loads is shown below.

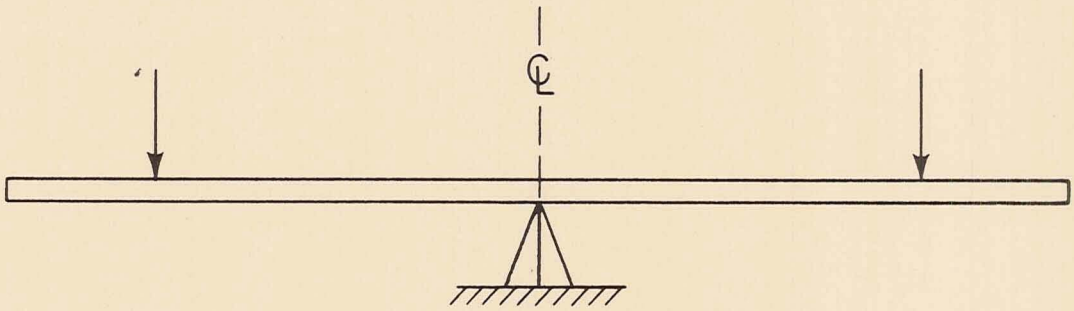

The method used to find the "fixed" influence coefficients requires that the deflections of the beam be determined at equal intervals. Also, if the beam has a continuous loading, then this continuous loading must be replaced by equivalent

concentrated loads placed at even intervals, ϵ, such as shown below.

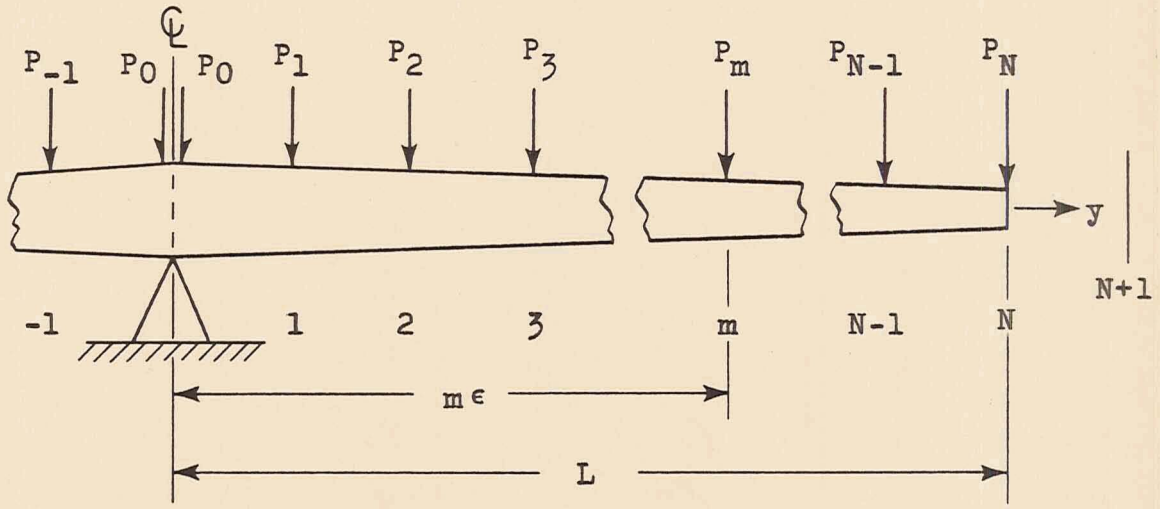

The "fixed" influence coefficients will be found by the method used by Stein and Sanders in reference 7. In this example, the power series for the deflection will only have one term and the expression for the total potential energy will only contain the energy of bending of the beam. If the beam is acted on by concentrated loads, then the total potential energy of the beam, π, is

$$\pi = \frac{1}{2}\int_0^L EI(y)(\eta'')^2 dy - \sum_{m=1}^{N} P_m \eta_m$$

The principle of minimum potential energy says that the deflection shape which satisfies equilibrium is the one for which π is a minimum. The method used by Stein and Sanders

to minimize π was first to replace the integration by a summation in accordance with the well-known trapezoidal rule. For this example, the total potential energy may now be written

$$\pi = \frac{\epsilon E}{2}\left[\frac{I_0}{2}(\eta_0'')^2 + I_1(\eta_1'')^2 + \ldots + I_m(\eta_m'')^2 + \ldots + \frac{I_N}{2}(\eta_N'')^2\right] - (P_1\eta_1 + \ldots + P_m\eta_m + \ldots + P_N\eta_N) \qquad (1)$$

If a parabolic curve is passed through the deflection curve, then the second derivative of the deflection at station 0 may be written in difference form as

$$\eta_0'' = \frac{\eta_{-1} - 2\eta_0 + \eta_1}{\epsilon^2}$$

but, since $\eta_{-1} = \eta_1$ and $\eta_0 = 0$

$$\eta_0'' = \frac{2\eta_1}{\epsilon^2}$$

For any station m the second derivative is

$$\eta_m'' = \frac{\eta_{m-1} - 2\eta_m + \eta_{m+1}}{\epsilon^2}$$

The above expressions for the second derivatives are now substituted into the expression for the total potential energy given by equation (1). This results in

$$\pi = \frac{E}{2\epsilon^3}\left[\frac{I_0}{2}(2\eta_1)^2 + I_1(-2\eta_1 + \eta_2)^2 + \ldots + I_m(\eta_{m-1} - 2\eta_m + \eta_{m+1})^2 + \ldots + \frac{I_N}{2}(\eta_{N-1} - 2\eta_N + \eta_{N+1})^2\right] - (P_1\eta_1 + \ldots + P_m\eta_m + \ldots + P_N\eta_N)$$

It should be noticed that replacing the second derivatives by differences introduces the deflection of the beam at one station past the tip into the energy expression.

The deflection shape which satisfies equilibrium is obtained by differentiating π with respect to each deflection and then setting the resulting equations equal to zero. Thus, for η_1

$$\frac{\partial \pi}{\partial \eta_1} = \frac{E}{2\epsilon^3}\left[\frac{8I_0}{2}\eta_1 - 4I_1(-2\eta_1 + \eta_2) + 2I_2(\eta_1 - 2\eta_2 + \eta_3)\right] - P_1 = 0$$

for η_m

$$\frac{\partial \pi}{\partial \eta_m} = \frac{E}{2\epsilon^3}\Big[2I_{m-1}(\eta_{m-2} - 2\eta_{m-1} + \eta_m) - 4I_m(\eta_{m-1} - 2\eta_m + \eta_{m+1}) + 2I_{m+1}(\eta_m - 2\eta_{m+1} + \eta_{m+2})\Big] - P_m = 0$$

and, for η_{N+1}

$$\frac{\partial \pi}{\partial \eta_{N+1}} = \frac{E}{2\epsilon^3}\Big[I_N(\eta_{N-1} - 2\eta_N + \eta_{N+1})\Big] = 0$$

The $N+1$ equations which result from the above minimization process can be written in the following matrix form

$$\begin{bmatrix} & & \\ & A & \\ & & \end{bmatrix} \begin{vmatrix} \eta_1 \\ \eta_2 \\ \vdots \\ \eta_m \\ \vdots \\ \eta_N \\ \eta_{N+1} \end{vmatrix} = \begin{vmatrix} P_1 \\ P_2 \\ \vdots \\ P_m \\ \vdots \\ P_N \\ 0 \end{vmatrix} \qquad (2)$$

where

$$\Big[A\Big] = \Big[D\Big]\Big[\frac{E}{\epsilon^3} I\Big]\Big[D\Big]'$$

in which (where the number of rows and columns are indicated on the right)

$$[D] = \begin{bmatrix} 2 & -2 & 1 & & & & & & \\ & 1 & -2 & 1 & & & & & \\ & & 1 & -2 & 1 & & & & \\ & & & \cdot & & & & & \\ & & & & \cdot & & & & \\ & & & & & \cdot & & & \\ & & & & & 1 & -2 & 1 & \\ & & & & & & 1 & -2 & 1 \\ & & & & & & & 1 & -2 \\ & & & & & & & & 1 \end{bmatrix} \quad (N+1) \times (N+1)$$

$$[D]' = \text{transpose of } [D]$$

$$\left[\frac{E}{\epsilon^3} I\right] = \frac{E}{\epsilon^3} \begin{bmatrix} \frac{I_0}{2} & & & & & & \\ & I_1 & & & & & \\ & & \cdot & & & & \\ & & & \cdot & & & \\ & & & & I_m & & \\ & & & & & \cdot & \\ & & & & & & \cdot \\ & & & & & & I_N \end{bmatrix} \quad (N+1) \times (N+1)$$

The A matrix in equation (2) is called the stiffness matrix since its coefficients give the load at one point necessary to cause a unit deflection at another point. However, what is wanted is the deflections in terms of the loads or the influence coefficient matrix. This matrix can be found by inverting the stiffness matrix. Multiplying

equation (2) by the inverse of the A matrix gives

$$\begin{Vmatrix} \eta_1 \\ \eta_2 \\ \vdots \\ \eta_m \\ \vdots \\ \eta_N \\ \eta_{N+1} \end{Vmatrix} = \begin{bmatrix} \\ A \\ \\ \end{bmatrix}^{-1} \begin{Vmatrix} P_1 \\ P_2 \\ \vdots \\ P_m \\ \vdots \\ P_N \\ 0 \end{Vmatrix} \qquad (3)$$

where A^{-1} is the influence coefficient matrix. The matrix equation (3) is a simultaneous set of equations which give the deflections in terms of the loads. Inasmuch as we are not interested in the deflection at the station past the tip, the last equation or the last row of equation (3) can be deleted. Also, the last column of the A^{-1} matrix can be omitted since this column is multiplied by the load at station N+1 which is zero. During a symmetric free-free vibration of the beam, the deflection of the center line, w_0, will not be zero. Thus, a place must be provided in the matrix equation for this deflection and its corresponding load P_0. Although at this time the deflection w_0 cannot be determined, it can be added to the matrix equation and its value determined later by considering the dynamic

equilibrium condition of the beam during a symmetric vibration. The deflection w_0 is added to matrix equation (3) by first adding a row and column of zeros so the first row and column of the A^{-1} matrix is zero, and then adding a column of w_0's to the right side of equation (3). After these operations and the operations to omit the deflection at station N+1 have been carried out, equation (3) may be written

$$\begin{vmatrix} w_0 \\ w_1 \\ \vdots \\ w_m \\ \vdots \\ w_N \end{vmatrix} = \begin{bmatrix} & & \\ & \Delta & \\ & & \end{bmatrix} \begin{vmatrix} P_0 \\ P_1 \\ \vdots \\ P_m \\ \vdots \\ P_N \end{vmatrix} + w_0 \begin{vmatrix} 1 \\ 1 \\ \vdots \\ 1 \\ \vdots \\ 1 \end{vmatrix}$$

or

$$\left| w \right| = \left[\Delta \right] \left| P \right| + w_0 \left| I \right| \qquad (4)$$

where Δ is derived from A^{-1} by deleting the last row and column and adding a row and column of zeros.

Up to this point, the deflections of the beam have been found in terms of concentrated static loads acting on

it. When the beam is in a natural vibration there will be no static loads, but there will be dynamic loads. These dynamic loads can be found by employing d'Alembert's principle which states that every state of motion may be considered at any instant as a state of equilibrium if appropriate inertia forces are introduced. The dynamic loads at any point y may now be written

$$p(y) = \omega^2 m(y) w(y)$$

The above equation gives the dynamic loads at any point of the beam. However, what is required for this analysis is the dynamic loads associated with each station. These loads can be found by concentrating the distributed mass of the beam at the stations.

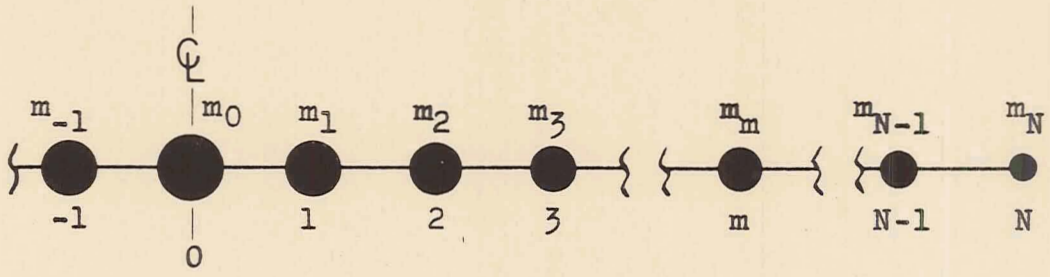

The dynamic load at any station m will be

$$P_m = \omega^2 m_m w_m \left(\frac{1}{1+\delta_{0m}}\right)$$

and if matrix notation is used, the dynamic loads at all the stations will be

$$\begin{Vmatrix} P_0 \\ P_1 \\ \vdots \\ P_m \\ \vdots \\ P_N \end{Vmatrix} = \omega^2 \begin{bmatrix} \frac{m_0}{2} & & & & & \\ & m_1 & & & & \\ & & \ddots & & & \\ & & & m_m & & \\ & & & & \ddots & \\ & & & & & m_N \end{bmatrix} \begin{Vmatrix} w_0 \\ w_1 \\ \vdots \\ w_m \\ \vdots \\ w_N \end{Vmatrix}$$

or

$$\left| P \right| = \omega^2 \left[M \right] \left| w \right| \tag{5}$$

If the dynamic loads given by equation (5) are substituted into equation (4), then the deflection of the beam in terms of the dynamic loads is found to be

$$\left| w \right| = \omega^2 \left[\Delta \right] \left[M \right] \left| w \right| + w_0 \left| I \right| \tag{6}$$

The unknown deflection, w_0, can be solved for by using the dynamic equilibrium condition that during free-free vibration

the sum of all the loads on the beam must be zero, or

$$\left\lfloor I \right\rfloor \left| P \right| = 0$$

which may also be written

$$\left\lfloor I \right\rfloor \left[M \right] \left| w \right| = 0$$

To apply this dynamic equilibrium condition, equation (6) is multiplied by the row matrix $\left\lfloor I \right\rfloor \left[M \right]$ and then set equal to zero. This yields

$$\omega^2 \left\lfloor I \right\rfloor \left[M \right] \left[\Delta \right] \left[M \right] \left| w \right| + w_0 \left\lfloor I \right\rfloor \left[M \right] \left| I \right| = 0$$

Now solving for w_0 from the above equation and substituting it into equation (6) gives

$$\left| w \right| = \omega^2 \left[\left[I \right] - \left| I \right| \frac{\left\lfloor I \right\rfloor \left[M \right]}{\left\lfloor I \right\rfloor \left[M \right] \left| I \right|} \right] \left[\Delta \right] \left[M \right] \left| w \right|$$

or

$$\left| w \right| = \omega^2 \left[C \right] \left[\Delta \right] \left[M \right] \left| w \right| \qquad (7)$$

where

$$\left[C\right] = \left[I\right] - \left|I\right| \frac{\left\lfloor I \right\rfloor \left[M\right]}{\left\lfloor I \right\rfloor \left[M\right] \left|I\right|}$$

The deflections and frequency for the first symmetric free-free mode of the beam can now be found by applying a matrix iteration to equation (7). In the matrix iteration, a normalized trial mode shape is substituted into the right hand side of equation (7), and the resulting mode shape on the left hand side found. This mode shape is then substituted into the right hand side and the left hand mode shape again found. This procedure is continued until the mode shape obtained on the left hand side is the same as the mode shape on the right hand side. The solution for the higher modes and frequencies can be found by using the well-known orthogonality condition that

$$\left\lfloor w_i \right\rfloor \left[M\right] \left| w_j \right| = 0$$

to sweep the lower mode components from the higher mode shapes. A method which does not need the orthogonality condition (and is therefore more generally applicable) is given by Wielandt in reference 9. Instead of an orthogonality relation, Wielandt used a linear combination of the

lower mode shapes in the sweeping process. A disadvantage of Wielandt's method is that although the frequencies are found directly, the mode shapes obtained are transformed modes or linear combinations of the lower mode shapes. If the actual mode shapes are wanted, then they can be obtained from the transformed modes.

CHAPTER V

CALCULATION OF THE THEORETICAL FREE-FREE MODES AND FREQUENCIES

Stein-Sanders Equations

In reference 7, Stein and Sanders have presented a method by which the influence coefficient matrix of a built-up delta wing can be determined. This matrix is obtained by inverting the stiffness matrix, which is given directly by the Stein-Sanders method. The stiffness matrix is found for a wing supported in two different conditions; these two support conditions are: (1) the wing rigidly clamped at the trailing edge of the center line with symmetrical loading, and (2) the wing simply supported at two points on the trailing edge with antisymmetrical loading (giving zero deflection along the center line). The stiffness matrix which is obtained for the wing in any one of these supported conditions is called the "fixed" stiffness matrix. Again, as was shown in the chapter "Discussion of Influence Coefficient Approach", the "fixed" stiffness matrix can be used to find the free-free natural modes and frequencies. The "fixed" stiffness matrix derived for the first condition is suitable for the symmetric free-free modes and the "fixed" stiffness matrix for the second condition is suitable for the antisymmetric free-free modes.

The deflections of the fixed wing are represented by the following power series of three terms

$$\eta(x,y) = \Phi_0(y) + x\Phi_1(y) + x^2\Phi_2(y) \qquad (8)$$

The coordinate system used to write equation (8) is shown in Figure 4. The physical meaning of the coefficients, or the generalized deflections, in the above power series is: $\Phi_0(y)$ represents the transverse displacement of the trailing edge, $\Phi_1(y)$ represents the twist of the wing, and $\Phi_2(y)$ represents the parabolic curvature in the chordwise direction. As in the example problem, the wing deflections are determined at a number of equally spaced stations along the span. For this wing, it is felt that station points located at every other rib are sufficient. This yields a value of the interval ϵ equal to 16 inches. The location and number of these station points is shown in Figure 5. Therefore, for the delta wing, the deflection shape at any spanwise station m is represented by a power series of the form

$$\eta(x,y_m) = \Phi_{0m} + x\Phi_{1m} + x^2\Phi_{2m} \qquad (9)$$

In the deflection analysis of a beam, the lateral loads enter into the equations simply as loads. However, in

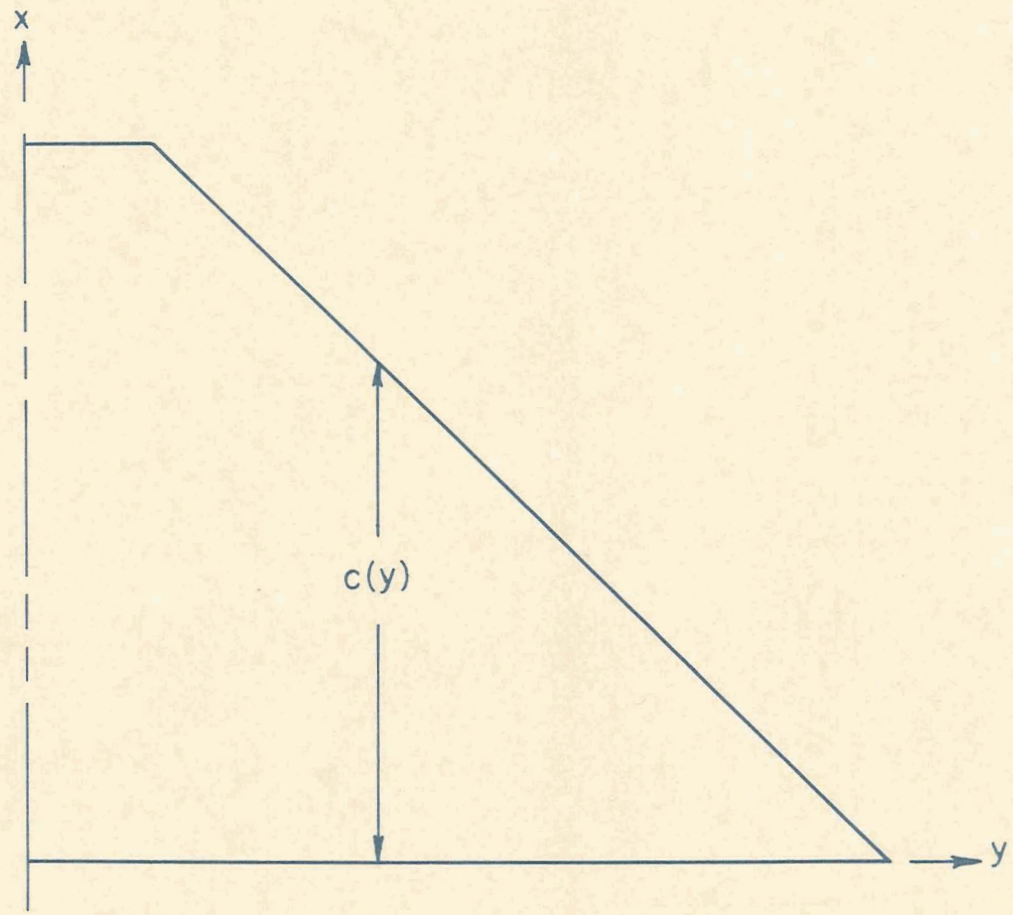

FIGURE 4

COORDINATE SYSTEM

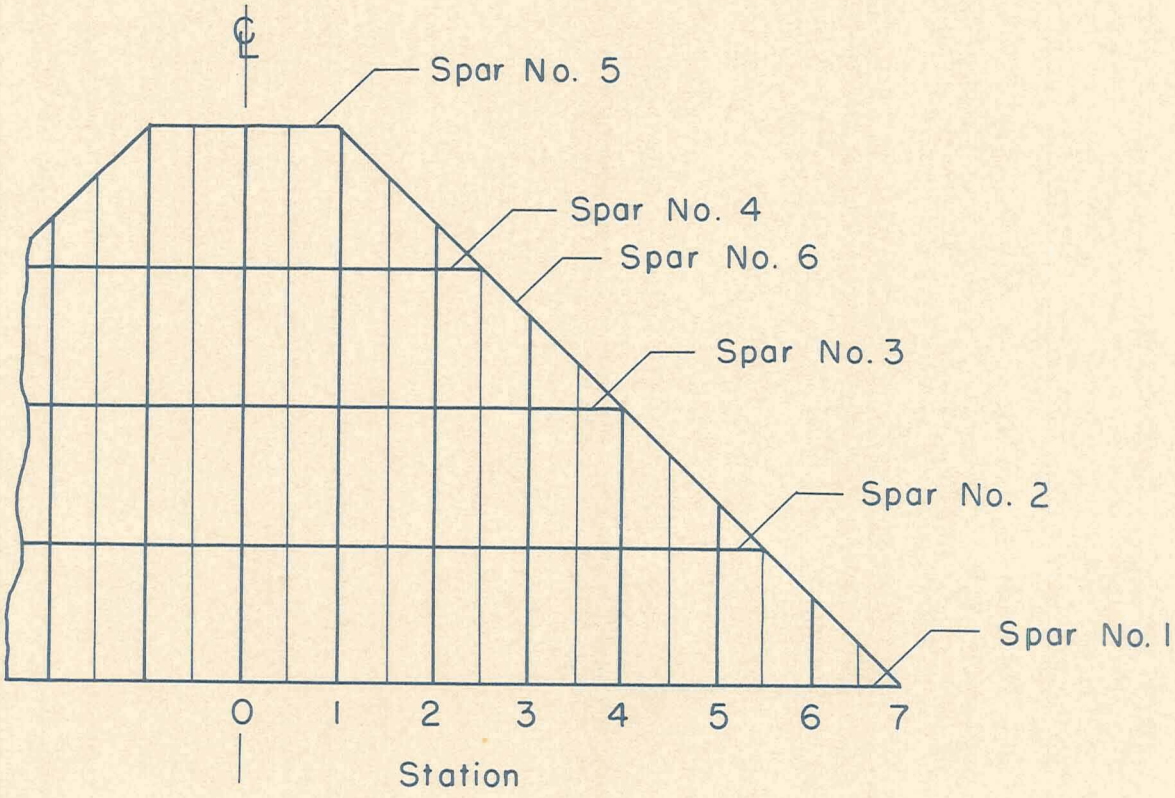

FIGURE 5

NUMBERING SYSTEM FOR STEIN-SANDERS METHOD

the Stein-Sanders method, the lateral loads which are distributed over the delta wing enter into the equations as loads, torques, and second moments. This is because the deflection shape is represented by a power series of three terms. If $p(x,y)$ is the distributed lateral load at any point x,y then the loads, torques, and second moments about the $x = 0$ axis may be written

$$p_n(y) = \int_0^{c(y)} p(x,y)x^{n-1}dx \tag{10}$$

where $p_n(y)$ is called the generalized load; $p_1(y)$ represents the load, $p_2(y)$ the torque, and $p_3(y)$ the second moment at station y. The generalized load defined by equation (10) is continuous over the span; however, the generalized loads used in the stiffness matrix are concentrated at the station points. For this reason, it is necessary to concentrate $p_n(y)$ at the station points. If the distance between station points is ϵ and if $p_n(y_m)$ is the value of $p_n(y)$ at station m, then the concentrated generalized loads at station m are

$$P_{nm} = \epsilon p_n(y_m)$$

The procedure used by Stein and Sanders to find the stiffness matrix was to first write the expression for the total potential energy of the built-up wing. The deflection shape given by equation (9) was then introduced into the total potential energy expression, and the derivatives of the Φ's written in difference form. The integration in the spanwise direction was then replaced by a summation in accordance with the trapezoidal rule. The minimization of the resulting total potential energy expression was then carried out. This resulted in a set of simultaneous algebraic equations in which the generalized deflections, Φ_{nm}, at the station points were related to generalized loads.

Symmetric "fixed" influence coefficient equation.- The "fixed stiffness matrix to be used to determine the symmetric modes and frequencies is found for a wing which is rigidly clamped at the trailing edge of the center line. A sketch of the wing clamped in this manner is shown in the following sketch.

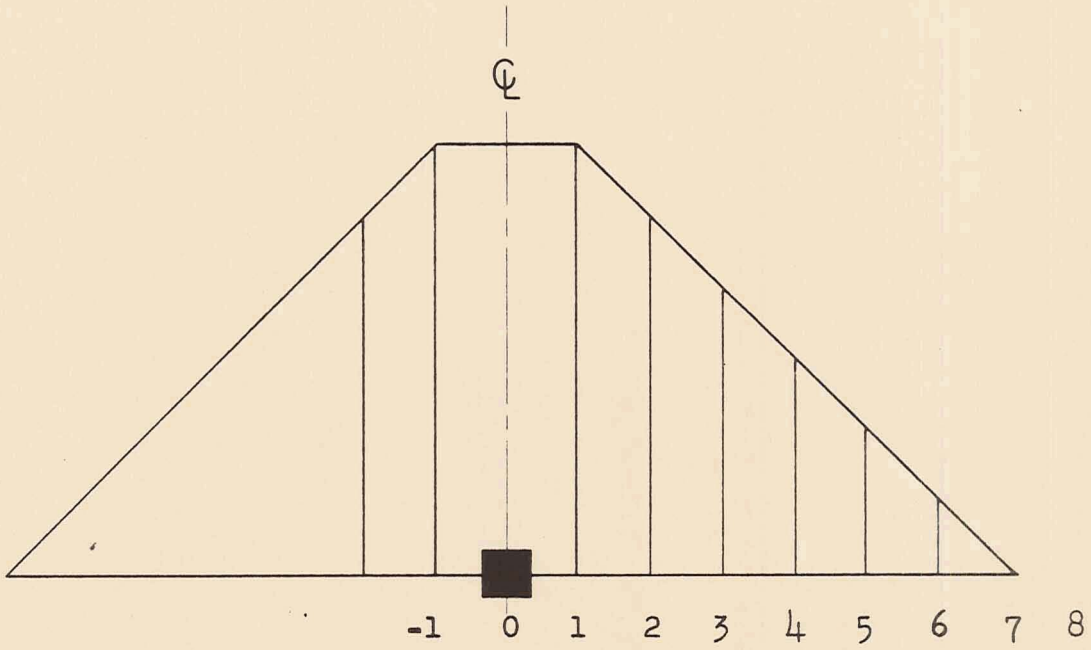

Now that the station points have been selected, the unknown generalized deflections in the matrix equation for the first condition are $\Phi_{01}, \ldots, \Phi_{08}, \Phi_{11}, \ldots, \Phi_{18}$, and $\Phi_{20}, \ldots, \Phi_{27}$; the known generalized loads are $P_{11}, \ldots, P_{17}, P_{21}, \ldots, P_{27}$, and $P_{31}, \ldots, P_{37}$. It should be noticed that although Φ_0, Φ_1, and Φ_2 at the station past the tip, station 8, appear in the original Stein-Sanders matrix equation, it is only necessary to use Φ_0 and Φ_1 at one station past the tip for this wing. This follows from the fact that the wing comes to a point at the tip; only these two quantities at station 8 are necessary to express completely the potential energy at the tip station.

With the above facts in mind, the Stein-Sanders matrix equation for the first condition may be written

$$\left[\begin{array}{c|c|c} & & \\ A_{11} & A_{12} & A_{13} \\ & & \\ \hline & & \\ A_{21} & A_{22} & A_{23} \\ & & \\ \hline & & \\ A_{31} & A_{32} & A_{33} \\ & & \end{array}\right] \left|\begin{array}{c} \Phi_{01} \\ \Phi_{02} \\ \vdots \\ \Phi_{07} \\ \Phi_{08} \\ \hline \Phi_{11} \\ \Phi_{12} \\ \vdots \\ \Phi_{17} \\ \Phi_{18} \\ \hline \Phi_{20} \\ \Phi_{21} \\ \vdots \\ \Phi_{27} \end{array}\right| = \left|\begin{array}{c} P_{11} \\ P_{12} \\ \vdots \\ P_{17} \\ 0 \\ \hline P_{21} \\ P_{22} \\ \vdots \\ P_{27} \\ 0 \\ \hline P_{30} \\ P_{31} \\ \vdots \\ P_{37} \end{array}\right|$$

or

$$\left[A_s\right] \left|\Phi\right| = \left|P\right| \qquad (11)$$

where, in the notation of the present paper

$$\left[A_{11}\right] = \left[D_1\right]\left[\left[a_1^{(1)}\right] + \left[\beta_s\right]\right]\left[D_1\right]'$$

$$\left[A_{12}\right] = \left[D_1\right]\left[\left[a_2^{(1)}\right]\left[D_1\right]' + \left[\beta_s\right]\left[X_s\right]'\right]$$

$$\left[A_{13}\right] = \left[D_1\right]\left[\left[a_3^{(1)}\right]\left[D_2\right]' + \left[\beta_s\right]\left[X_s^2\right]' + 2\mu\epsilon^2\left[a_1^{(2)}\right]\right]$$

$$\left[A_{22}\right] = \left[D_1\right]\left[a_3^{(1)}\right]\left[D_1\right]' + \left[X_s\right]\left[\beta_s\right]\left[X_s\right]' + 2(1-\mu)\epsilon^2\left[D_3\right]\left[a_1^{(3)}\right]\left[D_3\right]'$$

$$\left[A_{23}\right] = \left[D_1\right]\left[a_4^{(1)}\right]\left[D_2\right]' + \left[X_s\right]\left[\beta_s\right]\left[X^2\right]' + 4(1-\mu)\epsilon^2\left[D_3\right]\left[a_2^{(3)}\right]\left[D_4\right]' + 2\mu\epsilon^2\left[D_1\right]\left[a_2^{(2)}\right]$$

$$\left[A_{33}\right] = \left[D_2\right]\left[a_5^{(1)}\right]\left[D_2\right]' + \left[X_s^2\right]\left[\beta_s\right]\left[X^2\right]' + 8(1-\mu)\epsilon^2\left[D_4\right]\left[a_3^{(3)}\right]\left[D_4\right]' + 2\mu\epsilon^2\left[D_2\right]\left[a_3^{(2)}\right] + 2\mu\epsilon^2\left[\left[D_2\right]\left[a_3^{(2)}\right]\right]' + 4\epsilon^4\left[a_1^{(4)}\right] + \epsilon^3\left[r_s\right]$$

$$\left[A_{21}\right] = \left[A_{12}\right]'\ ;\ \left[A_{31}\right] = \left[A_{13}\right]'\ ;\ \left[A_{32}\right] = \left[A_{23}\right]'$$

The submatrices used in the above equations are defined in the following equations; the elements of the submatrices are defined after the definition of the submatrices.

$$[D_1] = \begin{bmatrix} 2 & -2 & 1 & & & & & & \\ & 1 & -2 & 1 & & & & & \\ & & 1 & -2 & 1 & & & & \\ & & & 1 & -2 & 1 & & & \\ & & & & 1 & -2 & 1 & & \\ & & & & & 1 & -2 & 1 & \\ & & & & & & 1 & -2 & \\ & & & & & & & 1 & \end{bmatrix}$$

$$[D_2] = \begin{bmatrix} -2 & 1 & & & & & & & \\ 2 & -2 & 1 & & & & & & \\ & 1 & -2 & 1 & & & & & \\ & & 1 & -2 & 1 & & & & \\ & & & 1 & -2 & 1 & & & \\ & & & & 1 & -2 & 1 & & \\ & & & & & 1 & -2 & 1 & \\ & & & & & & 1 & -2 & \\ & & & & & & & 1 & \end{bmatrix}$$

$$[D_3] = \begin{bmatrix} 1 & -1 & & & & & & \\ & 1 & -1 & & & & & \\ & & 1 & -1 & & & & \\ & & & 1 & -1 & & & \\ & & & & 1 & -1 & & \\ & & & & & 1 & -1 & \\ & & & & & & 1 & \\ & & & & & & 0 & \end{bmatrix}$$

$$[D_4] = \begin{bmatrix} -1 & & & & & & & \\ 1 & -1 & & & & & & \\ & 1 & -1 & & & & & \\ & & 1 & -1 & & & & \\ & & & 1 & -1 & & & \\ & & & & 1 & -1 & & \\ & & & & & 1 & -1 & \\ & & & & & & 1 & \\ & & & & & & 0 & \end{bmatrix}$$

$$\left[\overset{\nwarrow}{a_k^{(1)}}\right] = \begin{bmatrix} \frac{1}{2}a_{k0}^{*} & & & & & & \\ & a_{k1}^{*} & & & & & \\ & & \cdot & & & & \\ & & & \cdot & & & \\ & & & & a_{k6}^{*} & & \\ & & & & & a_{k7}^{*} \end{bmatrix} \qquad 8 \times 8$$

$$\left[a_k^{(2)}\right] = \begin{bmatrix} \frac{1}{2}a_{k0} & & & & & & \\ & a_{k1} & & & & & \\ & & \cdot & & & & \\ & & & \cdot & & & \\ & & & & a_{k5} & & \\ & & & & & a_{k6} & \\ & & & & & 0 & 0 \end{bmatrix} \qquad 8 \times 9$$

$$\left[\overset{\nwarrow}{a_k^{(3)}}\right] = \begin{bmatrix} a_{k,1/2} & & & & & & \\ & a_{k,3/2} & & & & & \\ & & \cdot & & & & \\ & & & \cdot & & & \\ & & & & a_{k,11/2} & & \\ & & & & & a_{k,13/2} \end{bmatrix} \qquad 7 \times 7$$

$$\left[\overset{\nwarrow}{a_1^{(4)}}\right] = \begin{bmatrix} \frac{1}{2}a_{10} & & & & & & \\ & a_{11} & & & & & \\ & & \cdot & & & & \\ & & & \cdot & & & \\ & & & & a_{15} & & \\ & & & & & a_{16} & \\ & & & & & 0 & \\ & & & & & & 0 \end{bmatrix} \qquad 9 \times 9$$

$$\left[\beta_s\right] = \begin{bmatrix} 0 & & & & & & & \\ & \frac{1}{2}\beta_1 & & & & & & \\ & & \beta_2 & & & & & \\ & & & \cdot & & & & \\ & & & & \cdot & & & \\ & & & & & \beta_6 & & \\ & & & & & & \frac{1}{2}\beta_7 & \end{bmatrix} \qquad 8 \times 8$$

$$
[\Gamma_s] = \begin{bmatrix}
\frac{B_0}{2} + \frac{B_{1/2}}{4} & \frac{B_{1/2}}{4} & & & & & & & \\
\frac{B_{1/2}}{4} & \frac{B_{1/2}}{4} + B_1 + \frac{B_{3/2}}{4} & \frac{B_{3/2}}{4} & & & & & & \\
 & \frac{B_{3/2}}{4} & \frac{B_{3/2}}{4} + B_2 + \frac{B_{3/2}}{4} & & & & & & \\
 & & & \ddots & & & & & \\
 & & & & & & & & \\
 & & & & & \frac{B_{11/2}}{4} + B_6 + \frac{B_{13/2}}{4} & \frac{B_{13/2}}{4} & \\
 & & & & & \frac{B_{13/2}}{4} & \frac{B_{13/2}}{4} & & 0
\end{bmatrix}
$$

9×9

$$[X_s] = \begin{bmatrix} \tilde{x}_{-1}+\tilde{x}_1 & -2\tilde{x}_1 & \tilde{x}_1 & & & & & \\ & \tilde{x}_2 & -2\tilde{x}_2 & \tilde{x}_2 & & & & \\ & & \tilde{x}_3 & -2\tilde{x}_3 & \tilde{x}_3 & & & \\ & & & \cdot & \cdot & \cdot & & \\ & & & & & \tilde{x}_6 & -2\tilde{x}_6 & \tilde{x}_6 \\ & & & & & & \tilde{x}_7 & -2\tilde{x}_7 \\ & & & & & & & \tilde{x}_8 \end{bmatrix} \qquad 8 \times 8$$

$$[X_s^2] = \begin{bmatrix} -2\tilde{x}_0^2 & \tilde{x}_0^2 & & & & & & \\ \tilde{x}_{-1}^2+\tilde{x}_1^2 & -2\tilde{x}_1^2 & \tilde{x}_1^2 & & & & & \\ & \tilde{x}_2^2 & -2\tilde{x}_2^2 & \tilde{x}_2^2 & & & & \\ & & & \cdot & \cdot & \cdot & & \\ & & & & & \tilde{x}_6^2 & -2\tilde{x}_6^2 & \tilde{x}_6^2 \\ & & & & & & \tilde{x}_7^2 & -2\tilde{x}_7^2 \\ & & & & & & & \tilde{x}_8^2 \end{bmatrix} \qquad 9 \times 8$$

The a_{ki}^* elements in the $a_k^{(1)}$ submatrix are made up of the stiffness properties of the straight spars (spars perpendicular to center line), cover sheet, and stringers. The equation for a_{ki}^* is

$$a_{ki}^* = \frac{E}{\epsilon^3}\left[\sum_{q=1}^{\tilde{N}_i} \tilde{I}_{qi}\tilde{x}_q^{k-1} + \frac{2tz_i^2}{1-\mu^2}\frac{c_i^k}{k} + \hat{I}_i \sum_{q=1}^{\hat{N}_i} \hat{x}_q^{k-1}\right]$$

where

ϵ = distance between spanwise stations (16 inch).

$\tilde{N}_i$ = number of straight spars at station i.

$\tilde{I}_{qi}$ = moment of inertia of the qth spar at station i, obtained from Table I. (Note: the moment of inertia of spars No. 1, 3, and 5 at stations 7, 4, and 1, respectively, should be half the value given in Table I. This is because these spars end at a station; thus, the interval over which the moment of inertia is summed should be $\frac{1}{2}\epsilon$ and not ϵ.)

$\tilde{x}_q$ = x coordinate of the qth spar.

t = cover sheet thickness (0.0696 inch).

z_i = cover sheet height, obtained from Table III.

c_i = chordwise length of cover sheet at station i.

$\hat{I}_i$ = moment of inertia of one stringer at station i, obtained from Table IV.

$\hat{N}_i$ = number of stringers (on both covers) at station i, obtained from Table IV.

$\hat{x}_q$ = x coordinate of the qth stringer, obtained from Figure 2.

The a^*_{ki}'s are tabulated in Table VIII for k = 1, 2, . . ., 5 and i = 0, 1, 2, . . ., 7.

TABLE VIII

ELEMENTS OF THE MATRICES DEFINED BY EQUATIONS (11) AND (13)

Station i	$\frac{a^*_{1i}}{E/\epsilon^3}$ in.^{4}	$\frac{a^*_{2i}}{E/\epsilon^3}$ in.^{5}	$\frac{a^*_{3i}}{E/\epsilon^3}$ in.^{6}	$\frac{a^*_{4i} \times 10^{-2}}{E/\epsilon^3}$ in.^{7}	$\frac{a^*_{5i} \times 10^{-4}}{E/\epsilon^3}$ in.^{8}	$\frac{\beta_i}{E/\epsilon^3}$ in.^{4}
0	187.151	8586.72	540,648	385,404	292,390	0
1	187.151	8586.72	540,648	385,404	292,390	0.813382
2	124.238	4764.39	250,464	148,058	93,508.9	.607404
3	77.5325	2417.80	103,551	49,642.3	25,334.2	.437386
4	42.3884	987.584	32,193.7	11,802.5	4,623.10	.300299
5	19.3926	289.985	6,174.39	1,469.67	372.193	.193115
6	5.98082	46.6473	506.866	61.2106	7.85371	.112809
7	.269720	0	0	0	0	.056350

Station i	$\frac{a_{1i}}{E/\epsilon^3}$ in.^{4}	$\frac{a_{2i}}{E/\epsilon^3}$ in.^{5}	$\frac{a_{3i}}{E/\epsilon^3}$ in.^{6}	$\frac{B_i}{4E/\epsilon^3}$ in.^{5}
0	110.833	5319.95	340,477	101.802
1/2	110.833	5319.95	340,477	101.802
1	110.833	5319.95	340,477	294.659
3/2	90.2631	3971.57	232,999	79.7650
2	72.3635	2894.54	154,375	61.4144
5/2	56.9509	2050.23	98,411.1	46.3320
3	43.8425	1402.96	59,859.7	34.1171
7/2	32.8557	919.960	34,345.2	24.3958
4	23.8077	571.384	18,284.3	16.8202
9/2	16.5156	330.313	8,808.34	11.0664
5	10.7969	172.750	3,685.34	6.83520
11/2	6.46871	77.6245	1,241.99	3.85008
6	3.34832	26.7866	285.724	1.86243
13/2	1.25300	5.01200	26.7307	.646000
7	0	0	0	0

The contribution of the cover sheet is given by a_{ki} where

$$a_{ki} = \frac{E}{\epsilon^3} \frac{2tz_i^2}{1 - \mu^2} \frac{c_i^k}{k}$$

The a_{ki}'s are tabulated in Table VIII for $k = 1, 2,$ and 3 and $i = 0, 1/2, 1, \ldots, 13/2, 7$.

The β_i's account for the stiffness properties of the leading edge spar and are defined as

$$\beta_i = \frac{E}{\epsilon^3} \tilde{I}_{6i} \cos^3\gamma$$

where

$\tilde{I}_{6i}$ = moment of inertia of the 6th spar at station i, obtained from Table I.

γ = angle that spar No. 6 makes with the center line (45°).

The β_i's are tabulated in Table VIII for $i = 1, 2, \ldots, 7$.

The rib stiffness is accounted for by the B_i element which is given by

$$B_i = \frac{4E}{\epsilon^3} \dot{I}_i c_i$$

where

I_i = moment of inertia of the rib located at station i, obtained from Table II.

The B_i's are tabulated in Table VIII for i = 0, 1/2, 1, . . ., 13/2, 7.

The $\tilde{x}_i$'s used in the X_s and X_s^2 submatrices are the x coordinate of spar No. 6.

It should be noticed that if the Stein-Sanders matrix equation were applied to a cantilever beam, then the resulting matrix equation would be identical to matrix equation (2) obtained in the chapter "Discussion of Influence Coefficient Approach." If the wing were only a beam, then equation (11) would reduce to

$$\left[A_{11}\right] \left|\Phi_0\right| = \left|P_1\right|$$

where, now

$$\left[A_{11}\right] = \left[D_1\right] \left[\frac{E}{\epsilon^3} I\right] \left[D_1\right]'$$

but, the D_1 matrix in equation (11) is the same as the D matrix used in equation (2), and Φ_0 is simply the deflection of the beam at the station points which is also the same as η.

The "fixed" influence coefficient matrix needed to find the symmetric modes and frequencies is found by inverting the A_s matrix in equation (11). The inversion of this 24×24 matrix was done by an IBM 604 automatic computing machine at Langley Field. The machine time required for the inversion was 9-1/2 hours. After equation (11) is multiplied through by the inverse of the A_s matrix, then this equation becomes

$$\begin{vmatrix} \Phi_{01} \\ \Phi_{02} \\ \vdots \\ \Phi_{07} \\ \Phi_{08} \\ \hline \Phi_{11} \\ \Phi_{12} \\ \vdots \\ \Phi_{17} \\ \Phi_{18} \\ \hline \Phi_{20} \\ \Phi_{21} \\ \vdots \\ \Phi_{27} \end{vmatrix} = \begin{bmatrix} \quad \\ \quad \\ \quad \\ \quad \\ \quad \\ \quad \\ \quad \\ A_s \\ \quad \\ \quad \\ \quad \\ \quad \\ \quad \\ \quad \\ \quad \end{bmatrix}^{-1} \begin{vmatrix} P_{11} \\ P_{12} \\ \vdots \\ P_{17} \\ 0 \\ \hline P_{21} \\ P_{22} \\ \vdots \\ P_{27} \\ 0 \\ \hline P_{30} \\ P_{31} \\ \vdots \\ P_{37} \end{vmatrix} \tag{12}$$

Equation (12) is called the symmetric "fixed" influence coefficient equation and gives the generalized deflection in terms of the generalized static loads of a wing which is rigidly clamped at the trailing edge of the center line.

Antisymmetric "fixed" influence coefficient equation.- To determine the "fixed" stiffness matrix of the wing in an antisymmetric free-free mode, the Stein-Sanders matrix equation for the second condition is used. The wing, supported in the manner of the second condition, is shown below.

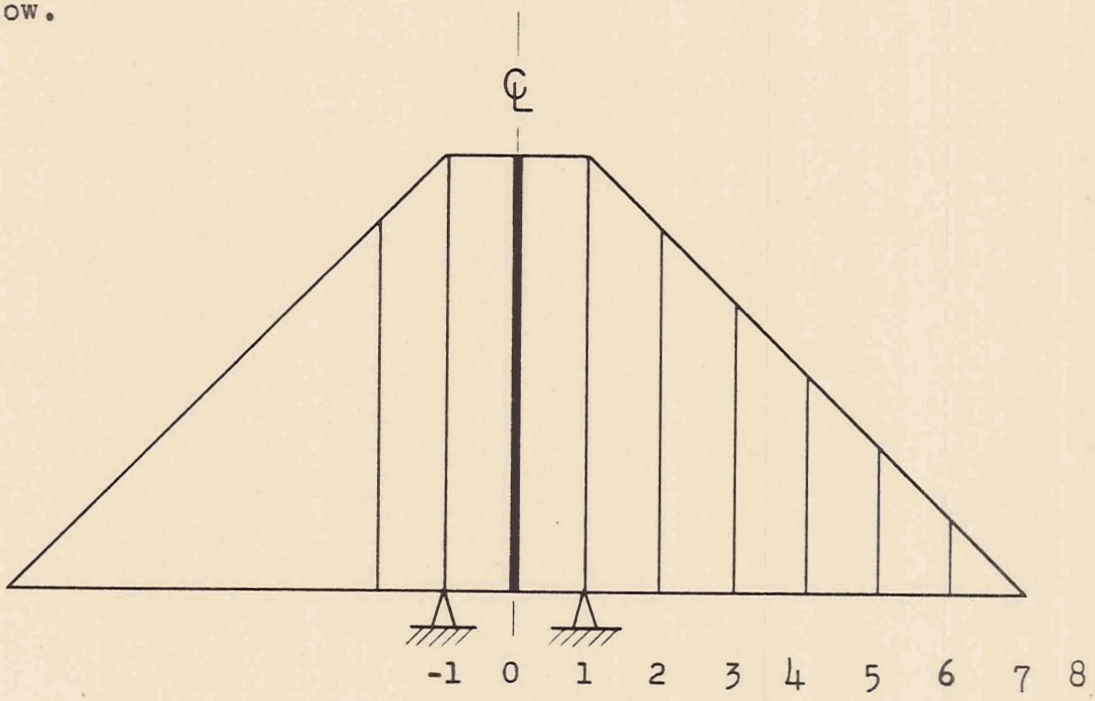

The unknown generalized deflections in the matrix equation for the second condition are $\Phi_{02}, \ldots, \Phi_{08}, \Phi_{11}, \ldots, \Phi_{18}$, and $\Phi_{21}, \ldots, \Phi_{27}$; the known generalized loads are

$P_{12}, \ldots, P_{17}, P_{21}, \ldots, P_{27}$, and $P_{31}, \ldots, P_{37}$. Again, the equation for Φ_{28} has been dropped because it is not necessary for this wing. Now the Stein-Sanders matrix equation for the second condition becomes

$$\left[\begin{array}{c|c|c} & & \\ A_{11} & A_{12} & A_{13} \\ & & \\ \hline & & \\ A_{21} & A_{22} & A_{23} \\ & & \\ \hline & & \\ A_{31} & A_{32} & A_{33} \\ & & \end{array}\right] \left|\begin{array}{c} \Phi_{02} \\ \Phi_{03} \\ \vdots \\ \Phi_{07} \\ \Phi_{08} \\ \hline \Phi_{11} \\ \Phi_{12} \\ \vdots \\ \Phi_{17} \\ \Phi_{18} \\ \hline \Phi_{21} \\ \Phi_{22} \\ \vdots \\ \Phi_{27} \end{array}\right| = \left|\begin{array}{c} P_{12} \\ P_{13} \\ \vdots \\ P_{17} \\ 0 \\ \hline P_{21} \\ P_{22} \\ \vdots \\ P_{27} \\ 0 \\ \hline P_{31} \\ P_{32} \\ \vdots \\ P_{37} \end{array}\right|$$

or

$$\left[A_a\right] \left| \Phi \right| = \left| P \right| \qquad (13)$$

where, in the notation of the present paper

$$[A_{11}] = [D_5]\left[\left[a_1^{(5)}\right] + [\beta_a]\right][D_5]'$$

$$[A_{12}] = [D_5]\left[\left[a_2^{(5)}\right][D_6]' + [\beta_a][X_a]'\right]$$

$$[A_{13}] = [D_5]\left[\left[a_3^{(5)}\right][D_6]' + [\beta_a]\left[X_a^2\right]' + 2\mu\epsilon^2\left[a_1^{(6)}\right]\right]$$

$$[A_{22}] = [D_6]\left[a_3^{(5)}\right][D_6]' + [X_a][\beta_a][X_a]' + 2(1-\mu)\epsilon^2[D_3]\left[a_1^{(3)}\right][D_3]'$$

$$[A_{23}] = [D_6]\left[a_4^{(5)}\right][D_6]' + [X_a][\beta_a]\left[X_a^2\right]' + 4(1-\mu)\epsilon^2[D_3]\left[a_2^{(3)}\right][D_3]' + 2\mu\epsilon^2[D_6]\left[a_2^{(6)}\right]$$

$$[A_{33}] = [D_6]\left[a_5^{(5)}\right][D_6]' + \left[X_a^2\right][\beta_a]\left[X_a^2\right]' + 8(1-\mu)\epsilon^2[D_3]\left[a_3^{(3)}\right][D_3]' + 2\mu\epsilon^2[D_6]\left[a_3^{(6)}\right] + 2\mu\epsilon^2\left[[D_6]\left[a_3^{(6)}\right]\right]' + 4\epsilon^4\left[a_1^{(7)}\right] + \epsilon^3[r_a]$$

$$[A_{21}] = [A_{12}]'\,;\quad [A_{31}] = [A_{13}]'\,;\quad [A_{32}] = [A_{23}]'$$

in which

$$[D_5] = \begin{bmatrix} 1 & -2 & 1 & & & & \\ & 1 & -2 & 1 & & & \\ & & 1 & -2 & 1 & & \\ & & & 1 & -2 & 1 & \\ & & & & 1 & -2 & 1 \\ & & & & & 1 & -2 \\ & & & & & & 1 \end{bmatrix}$$

$$[D_6] = \begin{bmatrix} -2 & 1 & & & & & \\ 1 & -2 & 1 & & & & \\ & 1 & -2 & 1 & & & \\ & & 1 & -2 & 1 & & \\ & & & 1 & -2 & 1 & \\ & & & & 1 & -2 & 1 \\ & & & & & 1 & -2 \\ & & & & & & 1 \end{bmatrix}$$

$$\left[a_k^{(5)}\right] = \begin{bmatrix} a^*_{k,1} & & & & & & \\ & a^*_{k,2} & & & & & \\ & & \cdot & & & & \\ & & & \cdot & & & \\ & & & & \cdot & & \\ & & & & & a^*_{k,6} & \\ & & & & & & a^*_{k,7} \end{bmatrix} \quad 7 \times 7$$

$$\left[a_k^{(6)}\right] = \begin{bmatrix} a_{k1} & & & & & & \\ & a_{k2} & & & & & \\ & & \cdot & & & & \\ & & & \cdot & & & \\ & & & & \cdot & & \\ & & & & & a_{k6} & \\ & & & & & & 0 \end{bmatrix} \quad 7 \times 7$$

$$\left[\overset{\nwarrow}{a_1}{}^{(7)}\overset{\searrow}{}\right] = \begin{bmatrix} a_{11} & & & & & & & \\ & a_{12} & & & & & & \\ & & \cdot & & & & & \\ & & & \cdot & & & & \\ & & & & \cdot & & & \\ & & & & & a_{16} & & \\ & & & & & & 0 & \\ & & & & & & & 0 \end{bmatrix} \qquad 8 \times 8$$

$$\left[\beta_a\right] = \begin{bmatrix} \frac{1}{2}\beta_1 & & & & & & \\ & \beta_2 & & & & & \\ & & \cdot & & & & \\ & & & \cdot & & & \\ & & & & \beta_6 & & \\ & & & & & \frac{1}{2}\beta_7 \end{bmatrix} \qquad 7 \times 7$$

$$\left[\Gamma_a\right] = \begin{bmatrix} \frac{B_{1/2}}{4} + B_1 + \frac{B_{3/2}}{4} & \frac{B_{3/2}}{4} & & & & & & \\ \frac{B_{3/2}}{4} & \frac{B_{3/2}}{4} + B_2 + \frac{B_{5/2}}{4} & \frac{B_{5/2}}{4} & & & & & \\ & \frac{B_{5/2}}{4} & \frac{B_{5/2}}{4} + B_3 + \frac{B_{7/2}}{4} & & & & & \\ & & & \ddots & & & & \\ & & & & \frac{B_{11/2}}{4} + B_6 + \frac{B_{13/2}}{4} & \frac{B_{13/2}}{4} & & \\ & & & & \frac{B_{13/2}}{4} & \frac{B_{13/2}}{4} + B_7 & & 0 \end{bmatrix}$$

8×8

$$\left[X_a\right] = \begin{bmatrix} -2\tilde{x}_1 & \tilde{x}_1 & & & & & & \\ \tilde{x}_2 & -2\tilde{x}_2 & \tilde{x}_2 & & & & & \\ & \tilde{x}_3 & -2\tilde{x}_3 & \tilde{x}_3 & & & & \\ & & \cdot & \cdot & \cdot & & & \\ & & & & \tilde{x}_6 & -2\tilde{x}_6 & \tilde{x}_6 & \\ & & & & & \tilde{x}_7 & -2\tilde{x}_7 & \\ & & & & & & \tilde{x}_8 & \end{bmatrix} \quad 8 \times 7$$

$$\left[X_a^2\right] = \begin{bmatrix} -2\tilde{x}_1^2 & \tilde{x}_1^2 & & & & & & \\ \tilde{x}_2^2 & -2\tilde{x}_2^2 & \tilde{x}_2^2 & & & & & \\ & \tilde{x}_3^2 & -2\tilde{x}_3^2 & \tilde{x}_3^2 & & & & \\ & & \cdot & \cdot & \cdot & & & \\ & & & & \tilde{x}_6^2 & -2\tilde{x}_6^2 & \tilde{x}_6^2 & \\ & & & & & \tilde{x}_7^2 & -2\tilde{x}_7^2 & \\ & & & & & & \tilde{x}_8^2 & \end{bmatrix} \quad 8 \times 7$$

The "fixed" influence coefficient matrix needed to find the antisymmetric modes and frequencies is found by inverting the A_a matrix in equation (13). The A_a matrix was also inverted on the IBM 604 machine. However, the machine time required was only 8 hours since A_a is a 22×22 matrix. After equation (13) is multiplied through

by the inverse of the A_a matrix, then this equation may be written

$$\begin{Bmatrix} \Phi_{02} \\ \Phi_{03} \\ \vdots \\ \Phi_{07} \\ \Phi_{08} \\ \hline \Phi_{11} \\ \Phi_{12} \\ \vdots \\ \Phi_{17} \\ \Phi_{18} \\ \hline \Phi_{21} \\ \Phi_{22} \\ \vdots \\ \Phi_{27} \end{Bmatrix} = \begin{bmatrix} & & \\ & A_a & \\ & & \end{bmatrix}^{-1} \begin{Bmatrix} P_{12} \\ P_{13} \\ \vdots \\ P_{17} \\ 0 \\ \hline P_{21} \\ P_{22} \\ \vdots \\ P_{27} \\ 0 \\ \hline P_{31} \\ P_{32} \\ \vdots \\ P_{37} \end{Bmatrix} \tag{14}$$

Equation (14) is called the antisymmetric "fixed" influence coefficient equation and gives the generalized deflections in terms of the generalized static loads of a wing which is simply supported at the station points 1 and -1 on the trailing edge and has zero deflection along the center line.

Discussion of "fixed" influence coefficient matrices.- The A_s^{-1} and A_a^{-1} matrices defined in equations (12) and (14), respectively, do not give the actual influence coefficients, that is, these coefficients do not relate the actual deflections to the actual static loads. What they do relate is the generalized deflections to the generalized loads. It is possible to modify A_s^{-1} and A_a^{-1} so that the actual deflections could be found in terms of the actual static loads. However, it is more convenient to work with the equations as they stand even though the dynamic loads acting on the wing will have to be modified so they are consistent with the generalized loads used in equations (12) and (14).

Free-Free Influence Coefficient Equations

The influence coefficients for the fixed wing were found in equations (12) and (14). In order to determine the free-free natural modes and frequencies of the wing, it is necessary to modify these "fixed" influence coefficients. This modification consists of making room in the influence coefficient matrix for the generalized deflections of the points which were considered fixed in deriving the "fixed" stiffness matrix.

The deflection of the wing in the fixed condition was denoted by $\eta(x,y_m)$; the deflection of the wing in the

free-free condition will be denoted by $w(x,y_m)$ where $w(x,y_m)$ is the deflection of the wing relative to the plane of rest and is represented by the following power series

$$w(x,y_m) = \Psi_{0m} + x\Psi_{1m} + x^2\Psi_{2m} \qquad (15)$$

In equation (15), Ψ_{0m} is the deflection of any station m on the trailing edge relative to the plane of rest, Ψ_{1m} represents the twist of the wing, and Ψ_{2m} represents the parabolic curvature in the chordwise direction. The relation between Φ_{0m} and Ψ_{0m}, for the symmetric case, is shown in the sketch below.

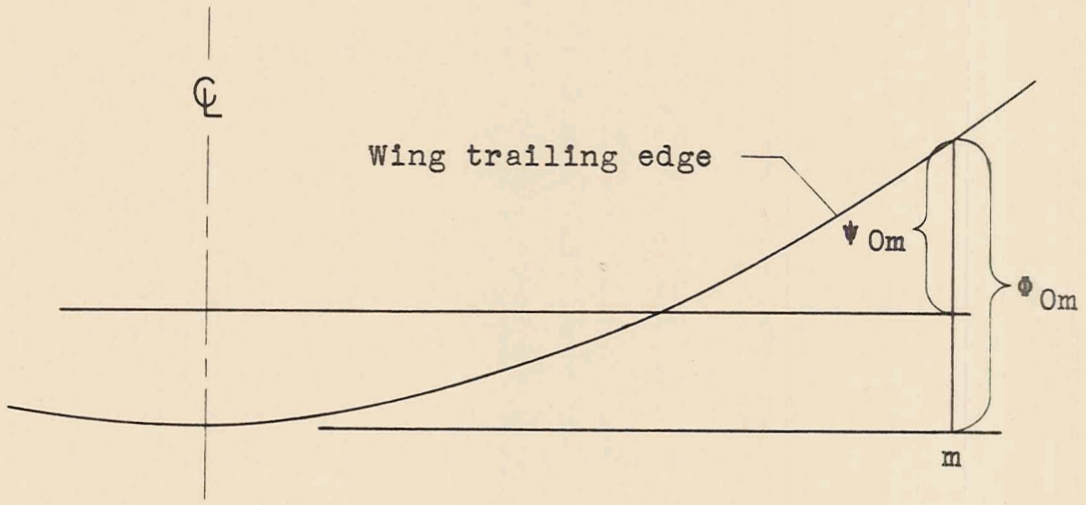

Symmetric free-free influence coefficient equation.- The influence coefficient matrix, A_s^{-1}, in equation (12) is for a wing which is rigidly clamped at the trailing edge of the center line. During a free-free symmetric vibration, the deflection and slope of the trailing edge of the center line will not be zero; thus, Ψ_{00}, Ψ_{10} and P_{10}, P_{20} must be added to equation (12). Although at this time, Ψ_{00} and Ψ_{10} cannot be added to equation (12), at least a place can be provided in the matrix equation so they can be added later. It should be noticed that the Φ's at one station past the tip, Φ_{08} and Φ_{18}, which were necessary in the original derivation of equation (11) are no longer necessary and the equations containing them can be deleted. This is the same procedure as that used in the chapter "Discussion of Influence Coefficient Approach." With these facts in mind, the following operations are now performed on the A_s^{-1} matrix:

1. The 8th and 16th row and column is deleted. This operation eliminates the equations for Φ_{08} and Φ_{18}.

2. Two rows and columns of zeros are added so the 1st and 9th row and column is zero. This is done to allow room for the Ψ_{00} and Ψ_{10} coefficients.

After these operations have been performed on the A_s^{-1} matrix, equation (12) becomes

$$\begin{vmatrix} 0 \\ \Phi_{01} \\ \vdots \\ \Phi_{06} \\ \Phi_{07} \\ \hline 0 \\ \Phi_{11} \\ \vdots \\ \Phi_{16} \\ \Phi_{17} \\ \hline \Phi_{20} \\ \Phi_{21} \\ \vdots \\ \Phi_{26} \\ \Phi_{27} \end{vmatrix} = \begin{bmatrix} & & \\ & \Delta_s & \\ & & \end{bmatrix} \begin{vmatrix} P_{10} \\ P_{11} \\ \vdots \\ P_{16} \\ P_{17} \\ \hline P_{20} \\ P_{21} \\ \vdots \\ P_{26} \\ P_{27} \\ \hline P_{30} \\ P_{31} \\ \vdots \\ P_{36} \\ P_{37} \end{vmatrix} \qquad (16)$$

where Δ_s is a 24×24 matrix and is the matrix that results after the previous operations on the A_s^{-1} matrix have been carried out. If the two unknown coefficients Ψ_{00} and Ψ_{10}

are added to the above equation, then equation (16) can be expressed as follows:

$$|\psi| = \left[\Delta_s\right] |P| + \psi_{00} |I_1| + \psi_{10} |I_2| \qquad (17)$$

where

$$|\psi| = \begin{vmatrix} \psi_{0i} \\ \hline \psi_{1i} \\ \hline \psi_{2i} \end{vmatrix}; \quad |P| = \begin{vmatrix} P_{1i} \\ \hline P_{2i} \\ \hline P_{3i} \end{vmatrix}; \quad |I_1| = \begin{vmatrix} I_8 \\ \hline 0 \\ \hline 0 \end{vmatrix}_{24 \times 1}; \quad |I_2| = \begin{vmatrix} 0 \\ \hline I_8 \\ \hline 0 \end{vmatrix}_{24 \times 1}$$

I_8 = column of 8 ones

$i = 0,1,2,\ldots, 7$

Equation (17 is called the symmetric free-free influence coefficient equation. To determine the modes and frequencies, it is now necessary to find the dynamic loads and the values of ψ_{00} and ψ_{10}.

Antisymmetric free-free influence coefficient equation.- The free-free influence coefficient matrix equation is obtained by appropriately modifying the "fixed" influence coefficient equation. (See eq. (14).) During a free-free antisymmetric vibration the deflection of the center line is zero, but there will be a deflection at the

station points 1 and -1 along the trailing edge. Thus, for the antisymmetric case, the coefficient Ψ_{01} and the corresponding loading term P_{11} must be added to the matrix equation for the influence coefficients. As in the symmetric case, equations for Φ_{08} and Φ_{18} are contained in equation (14) and now are no longer necessary.

The following operations are now performed on the A_a^{-1} matrix:

1. The 7th and 15th row and column is deleted. This operation eliminates the equations for Φ_{08} and Φ_{18}.

2. A row and column of zeros is added so the 1st row and column is zero. This is done to allow room for the Ψ_{01} coefficient.

After these operations have been performed on the A_a^{-1} matrix, equation (14) will take on the following form:

$$\left|\begin{array}{c} 0 \\ \Phi_{02} \\ \vdots \\ \Phi_{07} \\ \hline \Phi_{11} \\ \Phi_{12} \\ \vdots \\ \Phi_{17} \\ \hline \Phi_{21} \\ \Phi_{22} \\ \vdots \\ \Phi_{27} \end{array}\right| = \left[\begin{array}{c} \\ \\ \\ \\ \Delta_a \\ \\ \\ \\ \end{array}\right] \left|\begin{array}{c} P_{11} \\ P_{12} \\ \vdots \\ P_{17} \\ \hline P_{21} \\ P_{22} \\ \vdots \\ P_{27} \\ \hline P_{31} \\ P_{32} \\ \vdots \\ P_{37} \end{array}\right| \qquad (18)$$

where Δ_a is a 21 × 21 matrix and is the matrix that results after the previous operations on the A_a^{-1} matrix have been carried out. To obtain the free-free antisymmetric modes it is necessary to add a rigid body rotation about the x-axis to the above equation. After this is done, then equation (18) will become

$$|\psi| = \left[\Delta_a\right] |P| + \psi_{01}|r| \qquad (19)$$

where

$$|\psi| = \left|\begin{array}{c} \psi_{0j} \\ \hline \psi_{1j} \\ \hline \psi_{2j} \end{array}\right| ; \quad |P| = \left|\begin{array}{c} P_{1j} \\ \hline P_{2j} \\ \hline P_{3j} \end{array}\right| ; \quad |r| = \left|\begin{array}{c} 1 \\ 2 \\ \cdot \\ \cdot \\ \cdot \\ 7 \\ \hline 0 \\ \hline 0 \end{array}\right| \quad 21 \times 1$$

$$j = 1,2,\ldots,7$$

Equation (19) is called the antisymmetric free-free influence coefficient equation.

The Dynamic Loads

To determine the natural modes and frequencies of the delta wing specimen it is necessary to replace the static loads with dynamic loads. The dynamic loads at any point x,y on the wing may be written

$$p(x,y) = \omega^2 m(x,y) w(x,y) \tag{20}$$

In equation (20), $w(x,y)$ is the deflection of any point on the wing relative to the plane of rest and is represented by the following power series

$$w(x,y) = \psi_0(y) + x\psi_1(y) + x^2\psi_2(y) \tag{21}$$

If the expression for the deflection (eq. (21)) is substituted into equation (20), and the resulting equation for the dynamic loads substituted into equation (10), the following equation for the generalized dynamic loads at any station y is obtained:

$$p_n(y) = \omega^2 \int_0^{c(y)} m(x,y)\left[x^{n-1}\psi_0(y) + x^n\psi_1(y) + x^{n+1}\psi_2(y)\right]dx$$

Since the ψ's are independent of x, this equation may be written in the form

$$p_n(y) = \omega^2\left[m_n(y)\psi_0(y) + m_{n+1}(y)\psi_1(y) + m_{n+2}(y)\psi_2(y)\right] \quad (22)$$

where

$$m_k(y) = \int_0^{c(y)} m(x,y)x^{k-1}dx \quad (23)$$

Equation (22) gives the generalized dynamic loads at any spanwise station y. What is wanted is the generalized load at discrete spanwise station points. The procedure used to concentrate the distributed loads to the station points will be shown by considering only the loading due to the term

$$p_1(y) = \omega^2 m_1(y)\psi_0(y)$$

After the loading due to this term is found, it is easy to extend the results to the other terms in the equation for $p_n(y)$.

Let us consider first the distributed loads, $p_1^*(y)$, such as caused by the spars, cover sheet and stringers and then consider the concentrated loads, $\dot{p}_1(y)$, that result from the ribs being placed between the stations. To concentrate the distributed loads to a station point m, the mass per inch of the structure at station point m is multiplied by the distance between stations. This procedure is shown in the sketch below, where m^*_{1m} is the mass per inch at the mth station.

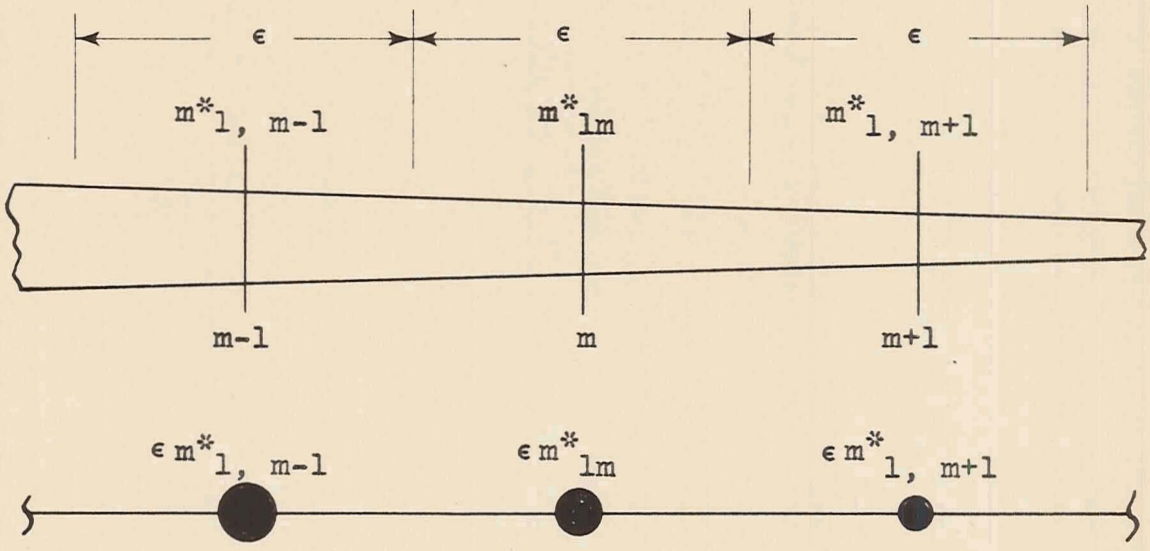

The generalized load P_l^* at station m will now be

$$P_{lm}^* = \omega^2 \epsilon\, m_{lm}^* \psi_{Om}$$

If there are 7 stations, then all the P_l^*'s can be written in matrix form as

$$\begin{Vmatrix} P_0^* \\ P_1^* \\ \vdots \\ P_6^* \\ P_7^* \end{Vmatrix} = \omega^2 \begin{bmatrix} & & \\ & M_l^* & \\ & & \end{bmatrix} \begin{Vmatrix} \psi_{00} \\ \psi_{01} \\ \vdots \\ \psi_{06} \\ \psi_{07} \end{Vmatrix}$$

where

$$\left[M_l^*\right] = \begin{bmatrix} \frac{1}{2} m_{l0}^* & & & & & & & \\ & m_{l1}^* & & & & & & \\ & & \ddots & & & & & \\ & & & \ddots & & & & \\ & & & & \ddots & & & \\ & & & & & m_{l6}^* & & \\ & & & & & & m_{l7}^* & \end{bmatrix} \qquad 8 \times 8$$

in which

$$m^*_{1i} = \epsilon \left[\sum_{q=1}^{\tilde{N}i} \tilde{m}_{qi} + 2\bar{m}c_i + \hat{m}\hat{N}_i \right]$$

$\tilde{N}_i$ = number of spars at station i (includes spar No. 6).

$\tilde{m}_{qi}$ = mass per inch of the qth spar at station i, obtained from Table I.

$\bar{m}$ = mass per square inch of the cover sheet (0.00696 lb/in.^{2}).

$\hat{m}$ = mass per inch of one stringer (0.01920 lb/in.).

When the m^*_{1i}'s were calculated, only one half of the mass of spar No. 1 at station 7, spar No. 3 at station 4 and spar No. 5 at station 1 was used. This was because these spars end at a station; thus, the interval over which the mass was summed should be $\frac{1}{2}\epsilon$ and not ϵ.

The calculation of $p_1^{\cdot}(y)$ for the ribs is complicated by the fact that not all the ribs lie on the stations. An approximation could be made by concentrating the ribs so their weight is on the station points. It is felt that this procedure does not adequately represent the actual mass distribution and consequently does not adequately represent the dynamic loads. Therefore, a method is presented which accounts for the ribs being placed between the stations. Again, the procedure for obtaining $\dot{P}_1$ due to Ψ_0 at

station m is shown, and then the results extended to the other ψ's and the other stations. If $\dot{m}_m$ is the mass of the rib at station m, then the location of the rib mass along the wing will look like

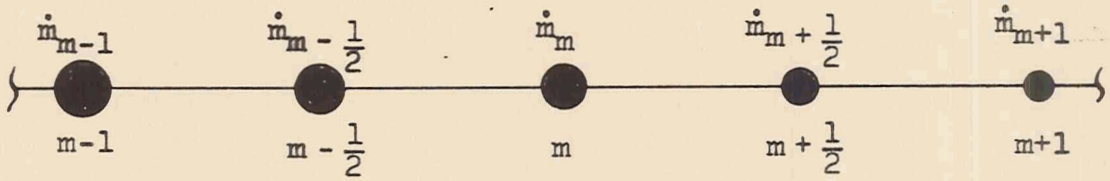

The contribution of the mass at station m to $\dot{P}_1$ will be

$$\omega^2 \dot{m}_m \psi_{0m}$$

If it is assumed that the deflection at the half stations can be obtained by a linear interpolation, then the contribution of the mass at the half station $m - \frac{1}{2}$ to $\dot{P}_1$ will be

$$\omega^2 \dot{m}_{m-\frac{1}{2}} \left(\frac{\psi_{0,m-1} + \psi_{0m}}{2} \right)$$

In the matrix equation, only the P's at the whole stations are used; thus, it is necessary to distribute the above contribution of the mass at the half station to a whole station. This is done by assuming that one half goes to the whole station on the left and the other half goes to the

whole station on the right. The equation for $\dot{P}_1$ at station m will now be

$$\dot{P}_{1m} = \omega^2 \left[\frac{1}{2}\dot{m}_m - \frac{1}{2}\left(\frac{\Psi_{0,m-1} + \Psi_{0m}}{2} \right) + \dot{m}_m \Psi_{0m} + \frac{1}{2}\dot{m}_m + \frac{1}{2}\left(\frac{\Psi_{0m} \quad \Psi_{0,m+1}}{2} \right) \right]$$

The equation for the $\dot{P}_1$'s due to the ribs at all the stations may now be written in matrix form as

$$\begin{vmatrix} \dot{P}_{10} \\ \dot{P}_{11} \\ \vdots \\ \dot{P}_{16} \\ \dot{P}_{17} \end{vmatrix} = \omega^2 \begin{bmatrix} \\ \\ \dot{M}_1 \\ \\ \\ \end{bmatrix} \begin{vmatrix} \Psi_{00} \\ \Psi_{01} \\ \vdots \\ \Psi_{06} \\ \Psi_{07} \end{vmatrix}$$

where $\dot{M}_1$ is defined on the next page. The mass of the rib at station i, $\dot{m}_i$, is obtained from Table II.

$$\left[\dot{M}_1\right] = \begin{bmatrix} \frac{\dot{m}_{10}}{2} + \frac{\dot{m}_{1,1/2}}{4} & \frac{\dot{m}_{1,1/2}}{4} & & & & & & \\ \frac{\dot{m}_{1,1/2}}{4} & \frac{\dot{m}_{1,1/2}}{4} + \dot{m}_{11} + \frac{\dot{m}_{1,3/2}}{4} & \frac{\dot{m}_{1,3/2}}{4} & & & & & \\ & \frac{\dot{m}_{1,3/2}}{4} & \frac{\dot{m}_{1,3/2}}{4} + \dot{m}_{12} + \frac{\dot{m}_{1,5/2}}{4} & \frac{\dot{m}_{1,5/2}}{4} & & & & \\ & & \cdot & \cdot & \cdot & & & \\ & & & & & \frac{\dot{m}_{1,11/2}}{4} + \dot{m}_{16} + \frac{\dot{m}_{1,13/2}}{4} & \frac{\dot{m}_{1,13/2}}{4} & \\ & & & & & \frac{\dot{m}_{1,13/2}}{4} & \frac{\dot{m}_{1,13/2}}{4} & \end{bmatrix}_{8 \times 8}$$

Now by combining the results just obtained, the equation for the P_1's for the spars, cover sheet, stringers, and ribs may be written

$$\left| P_{1i} \right| = \omega^2 \left[\left[M_1^* \right] + \left[\dot{M}_1 \right] \right] \left| \Psi_{0i} \right|$$

If a careful inspection is made of the expression for $p_n(y)$ given by equation (22), it is seen that the equation for the loads, torques and second moments at all the stations due to the spars, cover sheet and stringers will be

$$\left| \begin{array}{c} P_{1i}^* \\ \hline P_{2i}^* \\ \hline P_{3i}^* \end{array} \right| = \omega^2 \left[\begin{array}{c|c|c} M_1^* & M_2^* & M_3^* \\ \hline M_2^* & M_3^* & M_4^* \\ \hline M_3^* & M_4^* & M_5^* \end{array} \right] \left| \begin{array}{c} \Psi_{0i} \\ \hline \Psi_{1i} \\ \hline \Psi_{2i} \end{array} \right| \qquad (24)$$

where

$$\left[M_k^* \right] = \left[\begin{array}{cccccccc} \frac{1}{2} m_{k0}^* & & & & & & & \\ & m_{k1}^* & & & & & & \\ & & \cdot & & & & & \\ & & & \cdot & & & & \\ & & & & \cdot & & & \\ & & & & & m_{k6}^* & & \\ & & & & & & m_{k7}^* & \end{array} \right] \qquad 8 \times 8$$

in which

$$m^*_{ki} = \epsilon \left[\sum_{q=1}^{\tilde{N}i} \tilde{m}_{qi} x_q^{k-1} + 2\bar{m} \frac{c_i^k}{k} + \hat{m} \sum_{q=1}^{\hat{N}i} \hat{x}_q^{k-1} \right]$$

The m^*_{ki}'s are tabulated in Table IX for $k = 1, 2, \ldots, 5$ and $i = 0, 1, 2, \ldots, 7$.

In the discussion just presented to show the method of concentrating the dynamic loads which result from masses located between the station points, only the ribs were considered. But, it should be remembered that there are other concentrated masses located between the station points. These masses are the reinforcements, spar to rib rivets, shaker attachments, and pickups. These concentrated masses present no problem since they can be accounted for in the same manner as the ribs. If $\ddot{P}_{ni}$ represents the loads caused by the ribs and concentrated masses, then all the $\ddot{P}_{ni}$'s may be written

$$\begin{vmatrix} \ddot{P}_{1i} \\ \hline \ddot{P}_{2i} \\ \hline \ddot{P}_{3i} \end{vmatrix} = \omega^2 \left[\begin{array}{c|c|c} \ddot{M}_1 & \ddot{M}_2 & \ddot{M}_3 \\ \hline \ddot{M}_2 & \ddot{M}_3 & \ddot{M}_4 \\ \hline \ddot{M}_3 & \ddot{M}_4 & \ddot{M}_5 \end{array}\right] \begin{vmatrix} \Psi_{0i} \\ \hline \Psi_{1i} \\ \hline \Psi_{2i} \end{vmatrix} \qquad (25)$$

TABLE IX

ELEMENTS OF THE MATRIX DEFINED BY EQUATION (24)

Station i	m^*_{1i} lb	m^*_{2i} lb-in.	m^*_{3i} lb-in.^{2}	$m^*_{4i} \times 10^{-2}$ lb-in.^{3}	$m^*_{5i} \times 10^{-4}$ lb-in.^{4}
0	41.1278	1875.68	119,166	85,582.5	65,909.1
1	41.3244	1894.56	120,978	87,322.7	67,579.7
2	35.7325	1400.83	76,324.8	46,728.3	30,561.3
3	29.3469	932.372	41,296.1	20,420.0	10,741.3
4	22.3516	536.832	18,444.2	7,095.53	2,910.25
5	15.4279	240.865	5,521.20	1,395.06	372.152
6	7.40026	59.9939	720.445	95.4556	13.3428
7	1.82504	0	0	0	0

where $\ddot{M}_k$ is defined on the next page. The $\ddot{m}_{ki}$ elements in the $\ddot{M}_k$ matrix are

$$\ddot{m}_{ki} = \dot{m}_i \frac{c_i^{k-1}}{k} + \sum_{x_p=0,24,\ldots,96} m^{(c)}(x_p, y_i) x_p^{k-1}$$

where

$m^{(c)}(x_p, y_i)$ = concentrated mass at the point x_p, y_i, obtained from Tables V and VII

$$= \left(m^{(r)}(x_p, y_i) + m^{(t)}(x_p, y_i) \right).$$

The $\ddot{m}_{ki}$'s are tabulated in Table X for $k = 1, 2, \ldots, 5$ and $i = 0, 1/2, 1, \ldots, 13/2, 7$.

The equation for the dynamic loads due to the spars, cover sheet, stringers, ribs, reinforcements, spar to cover rivets, shaker attachments, and pickups is obtained by adding equations (24) and (25) so that

$$\left| \begin{array}{c} P_{1i} \\ \hline P_{2i} \\ \hline P_{3i} \end{array} \right| = \omega^2 \left[\quad M \quad \right] \left| \begin{array}{c} \Psi_{0i} \\ \hline \Psi_{1i} \\ \hline \Psi_{2i} \end{array} \right| \qquad (26)$$

$$\left[\ddot{M}_k\right] = \begin{bmatrix} \frac{\ddot{m}_{k,0}}{2} + \frac{\ddot{m}_{k,1/2}}{4} & \frac{\ddot{m}_{k,1/2}}{4} & & & & & & \\ \frac{\ddot{m}_{k,1/2}}{4} & \frac{\ddot{m}_{k,1/2}}{4} + \ddot{m}_{k1} + \frac{\ddot{m}_{k,3/2}}{4} & \frac{\ddot{m}_{k,3/2}}{4} & & & & & \\ & \frac{\ddot{m}_{k,3/2}}{4} & \frac{\ddot{m}_{k,3/2}}{4} + \ddot{m}_{k2} + \frac{\ddot{m}_{k,5/2}}{4} & \frac{\ddot{m}_{k,5/2}}{4} & & & & \\ & & \cdot & \cdot & \cdot & & & \\ & & & & & \frac{\ddot{m}_{k,11/2}}{4} + \ddot{m}_{k6} + \frac{\ddot{m}_{k,13/2}}{4} & \frac{\ddot{m}_{k,13/2}}{4} & \\ & & & & & \frac{\ddot{m}_{k,13/2}}{4} & \frac{\ddot{m}_{k,13/2}}{4} + \ddot{m}_{k7} & \end{bmatrix}$$

8×8

TABLE X

ELEMENTS OF THE MATRIX DEFINED BY EQUATION (25)

Station i	$\ddot{m}_{1i}$ lb	$\ddot{m}_{2i}$ lb-in.	$\ddot{m}_{3i}$ lb-in.^{2}	$\ddot{m}_{4i} \times 10^{-2}$ lb-in.^{3}	$\ddot{m}_{5i} \times 10^{-4}$ lb-in.^{4}
0	3.94690	211.262	14,982.9	11,847.3	9,917.19
1/2	3.46790	165.278	10,568.5	7,609.43	5,848.82
1	13.6952	667.504	44,861.0	33,857.2	27,255.5
3/2	2.99762	130.691	7,643.56	5,031.62	3,535.15
2	2.53836	100.768	5,364.99	3,213.82	2,054.36
5/2	6.25518	240.373	12,347.5	6,925.12	4,121.78
3	1.83293	58.2476	2,481.98	1,189.01	607.537
7/2	1.48624	41.4483	1,550.07	651.508	291.967
4	3.31127	79.3129	2,943.22	1,205.43	523.628
9/2	.920960	18.2723	486.674	145.685	46.5177
5	.684168	10.8864	232.725	55.8540	14.2820
11/2	3.17625	22.5150	495.184	113.423	26.4410
6	.284872	2.25625	24.0667	2.88801	.369665
13/2	.116360	.454080	2.42176	.145306	.0092995
7	.70	0	0	0	0

where

$$[M] = \left[\begin{array}{c|c|c} M_1 & M_2 & M_3 \\ \hline M_2 & M_3 & M_4 \\ \hline M_3 & M_4 & M_5 \end{array}\right]$$

$$[M_k] = [M_k^*] + [\ddot{M}_k]$$

Free-Free Modes and Frequencies

All that remains now to determine the natural modes and frequencies is to substitute the generalized dynamic loads into the free-free influence coefficient equations and determine the value of the unknown generalized deflections. This will yield a matrix equation from which the modes and frequencies can be found by applying a matrix iteration.

Symmetric free-free modes and frequencies.- To obtain the matrix equation which yields the symmetric free-free modes and frequencies, the dynamic loads given by equation (26) are first substituted into the symmetric free-free influence coefficient equation (eq. (17)) this yields

$$|\psi| = \omega^2[\Delta_s][M]\,|\psi| + \psi_{00}\,|I_1| + \psi_{10}\,|I_2| \qquad (27)$$

The ψ_{00} and ψ_{10} can be solved for by considering the dynamic equilibrium conditions which the symmetric free-free

wing must satisfy. One dynamic equilibrium condition is that the sum of all the dynamic loads must be zero

$$\sum_{i=0}^{7} P_{1i} = 0 \tag{28}$$

The other dynamic equilibrium condition is that the sum of the moments of all the dynamic loads about the y-axis must be zero

$$\sum_{i=0}^{7} P_{2i} = 0 \tag{29}$$

Equations (28) and (29) may be written in matrix form as

$$\lfloor I_1 \rfloor \, | P | = 0$$

or (28a)

$$\lfloor I_1 \rfloor \, [M] \, | \psi | = 0$$

and

$$\lfloor I_2 \rfloor \, | P | = 0$$

or (29a)

$$\lfloor I_2 \rfloor \, [M] \, | \psi | = 0$$

When the dynamic equilibrium condition given by equation (28a) is applied to equation (27), the following relation is obtained

$$\omega^2 \left[I_1\right]\left[M\right]\left[\Delta_s\right]\left[M\right]\left|\psi\right| + \psi_{00}\left[I_1\right]\left[M\right]\left|I_1\right| + \psi_{10}\left[I_1\right]\left[M\right]\left|I_2\right| = 0$$

and when the dynamic equilibrium condition given by equation (29a) is applied to equation (27)

$$\omega^2 \left[I_2\right]\left[M\right]\left[\Delta_s\right]\left[M\right]\left|\psi\right| + \psi_{00}\left[I_2\right]\left[M\right]\left|I_1\right| + \psi_{10}\left[I_2\right]\left[M\right]\left|I_2\right| = 0$$

The above two equations may be written in the following matrix form

$$\begin{bmatrix} m_{11} & m_{12} \\ m_{12} & m_{22} \end{bmatrix} \begin{vmatrix} \psi_{00} \\ \psi_{10} \end{vmatrix} = -\omega^2 \begin{bmatrix} \left[I_1\right] \\ \left[I_2\right] \end{bmatrix} \left[M\right]\left[\Delta_s\right]\left[M\right]\left|\psi\right|$$

where

$$\begin{aligned} m_{11} &= \left[I_1\right]\left[M\right]\left|I_1\right| \qquad m_{22} = \left[I_2\right]\left[M\right]\left|I_2\right| \\ m_{12} &= \left[I_1\right]\left[M\right]\left|I_2\right| \end{aligned} \tag{30}$$

Now solving for ψ_{00} and ψ_{10} yields

$$\psi_{00} = \omega^2 \left|\alpha_{22}\left[I_1\right] - \alpha_{12}\left[I_2\right]\right|\left[M\right]\left[\Delta_s\right]\left[M\right]\left|\psi\right|$$

and

$$\psi_{10} = \omega^2 \left[\alpha_{11} \left[I_2 \right] - \alpha_{12} \left[I_1 \right] \right] \left[M \right] \left[\Delta_s \right] \left[M \right] \left| \psi \right|$$

where

$$\alpha_{11} = \frac{m_{11}}{m_{12}^2 - m_{11} m_{22}}; \quad \alpha_{12} = \frac{m_{12}}{m_{12}^2 - m_{11} m_{22}}; \quad \alpha_{22} = \frac{m_{22}}{m_{12}^2 - m_{11} m_{22}} \tag{31}$$

Now that the values of ψ_{00} and ψ_{10} which satisfy the dynamic equilibrium conditions have been obtained, it is necessary to substitute them into equation (27). This gives

$$\left| \psi \right| = \omega^2 \left[\left[I_s \right] + \left[\alpha_{22} \left| I_1 \right| \left[I_1 \right] - \alpha_{12} \left| I_1 \right| \left[I_2 \right] + \alpha_{11} \left| I_2 \right| \left[I_2 \right] - \alpha_{12} \left| I_2 \right| \left[I_1 \right] \right] \left[M \right] \right] \left[\Delta_s \right] \left[M \right] \left| \psi \right|$$

or

$$\left| \psi \right| = \omega^2 \left[C_s \right] \left[\Delta_s \right] \left[M \right] \left| \psi \right| \tag{32}$$

where I_s is a 24×24 unit matrix. Although equation (32) is correct as it stands, it may be written in a simplier form. If the C_s matrix is written

$$\left[C_s\right] = \left[I_s\right] + \left[D_s\right]$$

then the D_s matrix may be written, after simplification

$$
\left[D_s\right] = \left[\begin{array}{c|c|c}
\left|1_8\right|\left[\alpha_{22}\left[m_1\right] - \alpha_{12}\left[m_2\right]\right] & \left|1_8\right|\left[\alpha_{22}\left[m_2\right] - \alpha_{12}\left[m_3\right]\right] & \left|1_8\right|\left[\alpha_{22}\left[m_3\right] - \alpha_{12}\left[m_4\right]\right] \\
\hline
\left|1_8\right|\left[\alpha_{11}\left[m_2\right] - \alpha_{12}\left[m_1\right]\right] & \left|1_8\right|\left[\alpha_{11}\left[m_3\right] - \alpha_{12}\left[m_2\right]\right] & \left|1_8\right|\left[\alpha_{11}\left[m_4\right] - \alpha_{12}\left[m_3\right]\right] \\
\hline
0 & 0 & 0
\end{array}\right] \qquad 24 \times 24
$$

where

$$\lfloor m_k \rfloor = \lfloor I_8 \rfloor \lfloor M_k \rfloor$$

By using the above notation, the m_{11}, m_{12} and m_{22} parameters defined by equation (30) may be written

$$m_{11} = \lfloor m_1 \rfloor \, |I_8| ; \; m_{12} = \lfloor m_2 \rfloor \, |I_8| ; \; m_{22} = \lfloor m_3 \rfloor \, |I_8|$$

The symmetric free-free modes and frequencies are now found by applying a matrix iteration to equation (32). For this process, an IBM CPC automatic computing machine was used. The first four modes and frequencies were found. The machine performed each iteration in 5 minutes. For the first mode, 15 iterations were used, for the second, 25 iterations, for the third, 35 iterations, and for the fourth mode, 50 iterations were used. Since Wielandt's sweeping method was used for the second, third and fourth modes, the mode shapes obtained in the matrix iteration were transformed modes. To obtain the true modes, an IBM 604 machine was used.

Antisymmetric free-free modes and frequencies.- The antisymmetric free-free modes and frequencies are found by substituting the dynamic loads into equation (19), determining

the unknown coefficient Ψ_{01}, by considering the dynamic equilibrium condition, and then applying a matrix iteration to the resulting equation. The expression for the anti-symmetric dynamic loads is obtained from equation (26) by striking out the 1st, 9th and 17th row and column of the M matrix. This yields the following matrix equation for the antisymmetric dynamic loads

$$\left|\begin{array}{c} P_{1j} \\ \hline P_{2j} \\ \hline P_{3j} \end{array}\right| = \omega^2 \left[\begin{array}{c} \\ M_a \\ \\ \end{array}\right] \left|\begin{array}{c} \Psi_{0j} \\ \hline \Psi_{1j} \\ \hline \Psi_{2j} \end{array}\right| \qquad (33)$$

where

$$j = 1, 2, \ldots, 7$$

The substitution of equation (33) into equation (19) yields

$$\left|\Psi\right| = \omega^2 \left[\Delta_a\right]\left[M_a\right]\left|\Psi\right| + \Psi_{01}\left|r\right| \qquad (34)$$

The dynamic equilibrium condition for the anti-symmetric case is that the sum of the moments of the dynamic loads about the x-axis must be zero

$$\sum_{j=1}^{7} y_j P_{1j} = 0$$

This equation can be written in matrix form as

$$\lfloor r \rfloor \left| P \right| = 0$$

or, by using equation (33)

$$\lfloor r \rfloor \left[M_a \right] \left| \psi \right| = 0 \tag{35}$$

If the equation for ψ (eq. (34)) is introduced into equation (35), then the dynamic equilibrium condition for the antisymmetric case becomes

$$\omega^2 \lfloor r \rfloor \left[M_a \right] \left[\Delta_a \right] \left[M_a \right] \left| \psi \right| + \psi_{01} \lfloor r \rfloor \left[M_a \right] \left| r \right| = 0$$

Solving for ψ_{01} from the above equation and substituting it into equation (34) yields

$$\left| \psi \right| = \omega^2 \left[\left[I_a \right] - \frac{\left| r \right| \lfloor r \rfloor \left[M_a \right]}{\lfloor r \rfloor \left[M_a \right] \left| r \right|} \right] \left[\Delta_a \right] \left[M_a \right] \left| \psi \right|$$

or

$$\left| \psi \right| = \omega^2 \left[C_a \right] \left[\Delta_a \right] \left[M_a \right] \left| \psi \right| \tag{36}$$

where I_a is a 21 × 21 unit matrix. After a few manipulations, the C_a matrix may be written

$$\left[C_a\right] = \left[I_a\right] - \frac{1}{\left[\bar{r}\right]\left[M_1\right]\left|\bar{r}\right|} \left[\begin{array}{c|c|c} \left[R\right]\left[M_1\right] & \left[R\right]\left[M_2\right] & \left[R\right]\left[M_3\right] \\ \hline 0 & 0 & 0 \\ \hline 0 & 0 & 0 \end{array}\right]$$

where

$$\left|\bar{r}\right| = \left[1\ 2\ 3\ 4\ 5\ 6\ 7\right]$$
$$\left[R\right] = \left|\bar{r}\right|\left[\bar{r}\right]$$

Now by using the above value of C_a in equation (36), the antisymmetric free-free modes and frequencies of the wing can be determined by using a matrix iteration. As in the symmetrical case, automatic computing machines were used to carry out the matrix iteration. Approximately the same number of iterations were required for the antisymmetric case as were required for the symmetric case.

Discussion of parameters.- At this point, the physical significance of the m_{11}, m_{12} and m_{22} parameters defined by equation (30) should be brought out. The m_{11} parameter is simply the mass of one half of the wing, the m_{12} parameter is the moment of the mass about the y-axis, and the m_{22} parameter is the second moment of the mass about the y-axis. The center of gravity of the wing is simply m_{12}/m_{11}.

The weight and center of gravity of the wing were determined by measurements. A comparison of the measured and calculated m's is shown below.

	Measured	Calculated
$2m_{11}$, lb	435.2	433.242
$2m_{12}$, lb-in.		15,316.8
$2m_{22}$, lb-in.^{2}.		840,930
center of gravity, in.	35.5	35.36

Comparison With Experimental Results

The theoretical natural free-free modes and frequencies of the built-up delta wing specimen were obtained by applying a matrix iteration to equation (32), for the symmetric modes and frequencies, and to equation (36), for the antisymmetric modes and frequencies. The first four frequencies obtained from these equations along with the experimental frequencies and the percentage error are listed on the next page.

Symmetric Frequencies				Antisymmetric Frequency			
Mode	Exp. freq. cps	Theor. freq. cps	% error	Mode	Exp. freq. cps	Theor. freq. cps	% error
1st	43.3	46.38	7.12	1st	52.2	56.70	8.43
2nd	88.8	105.3	18.58	2nd	91.7	103.4	12.77
3rd	122.8	149.9	22.05	3rd	131.1	166.6	27.08
4th	164.2	210	27.72	4th	169.2	216.5	27.95

The mode shapes as well as the frequencies were obtained in the matrix iteration. However, the mode shapes obtained from the matrix iteration were the Ψ coefficients. These coefficients, for the first four symmetric and antisymmetric modes, are tabulated in Table XI.

The node lines were found by setting the deflection equal to zero and solving for the chordwise location of zero deflection, or the following equation was solved for x

$$\Psi_{0m} + x\Psi_{1m} + x^2\Psi_{2m} = 0$$

A plot of the theoretical and experimental node lines for the symmetric modes is given in Figure 6 and for the antisymmetric modes in Figure 7.

TABLE XI

THE Ψ COEFFICIENTS FOR SYMMETRIC AND ANTISYMMETRIC MODES

Station i	First symmetric mode			First antisymmetric mode			Second symmetric mode			Second antisymmetric mode		
	Ψ_{0i}	$\Psi_{1i} \times 10^2$	$\Psi_{2i} \times 10^4$	Ψ_{0i}	$\Psi_{1i} \times 10^2$	$\Psi_{2i} \times 10^4$	Ψ_{0i}	$\Psi_{1i} \times 10^2$	$\Psi_{2i} \times 10^4$	Ψ_{0i}	$\Psi_{1i} \times 10^2$	$\Psi_{2i} \times 10^4$
0	-1.4965	2.4599	-0.5541	0	0	0	0.7358	-1.7959	1.4878	0.	0	0
1	-1.3885	2.3452	- .5397	-0.0312	0.5752	0.0017	.6889	-1.8697	1.5642	0.3181	-0.6477	- 0.0030
2	-1.0724	2.0242	- .5249	- .1154	1.3131	- .1392	.5644	-2.1403	1.8523	.6018	-1.3888	.1913
3	- .5262	1.5006	- .5695	- .2687	2.1039	- .2562	.3644	-2.5116	2.1927	.7396	-1.9110	.4005
4	.2606	.7709	- .7284	- .5137	2.8935	- .2058	.1214	-2.9068	2.3618	.6272	-1.9885	.5835
5	1.2694	- .1266	-1.0453	- .8625	3.6493	.1118	- .1112	-3.2928	2.0978	.1908	-1.4828	.8543
6	2.4402	-1.1842	- .9527	-1.2995	4.3408	.6029	- .2907	-3.5689	.6951	- .5527	- .4515	1.4013
7	3.6945	-1.5109	-6.8700	-1.7963	4.5575	5.0698	- .3899	-3.8409	-3.2428	-1.5264	.3366	10.0000

Station i	Third symmetric mode			Third antisymmetric mode			Fourth symmetric mode			Fourth antisymmetric mode		
	Ψ_{0i}	$\Psi_{1i} \times 10^2$	$\Psi_{2i} \times 10^4$	Ψ_{0i}	$\Psi_{1i} \times 10^2$	$\Psi_{2i} \times 10^4$	Ψ_{0i}	$\Psi_{1i} \times 10^2$	$\Psi_{2i} \times 10^4$	Ψ_{0i}	$\Psi_{1i} \times 10^2$	$\Psi_{2i} \times 10^4$
0	-0.1201	-0.9259	1.5852	0	0	0	-1.0419	6.0315	- 6.1120	0	0	0
1	- .0367	-1.1028	1.6473	-0.0643	-0.1502	0.0042	- .9018	5.4315	- 5.5649	-0.0964	0.2070	-0.0012
2	.1792	-1.5427	1.7752	- .1578	.2960	- .6281	- .4795	3.4143	- 3.6438	- .1062	.0798	.2517
3	.4345	-1.9438	1.7217	- .2096	1.2590	- 1.8514	.1194	.0047	- .2265	- .0097	- .3736	.6835
4	.5669	-1.9540	1.3760	- .2107	2.6305	- 3.3897	.6753	-4.1625	4.0920	.1522	- .9523	1.0543
5	.3694	-1.2223	.9849	- .2266	4.1626	- 4.3593	.8517	-7.4643	7.3826	.2373	-1.1913	1.0629
6	- .2817	.2893	1.7277	- .3680	5.3467	- 2.1608	.4059	-7.9363	6.1574	.0574	- .5948	.9922
7	-1.3968	1.9031	16.1250	- .7626	6.2547	10.0000	- .6284	-6.0465	10.0000	- .5128	.7359	9.6160

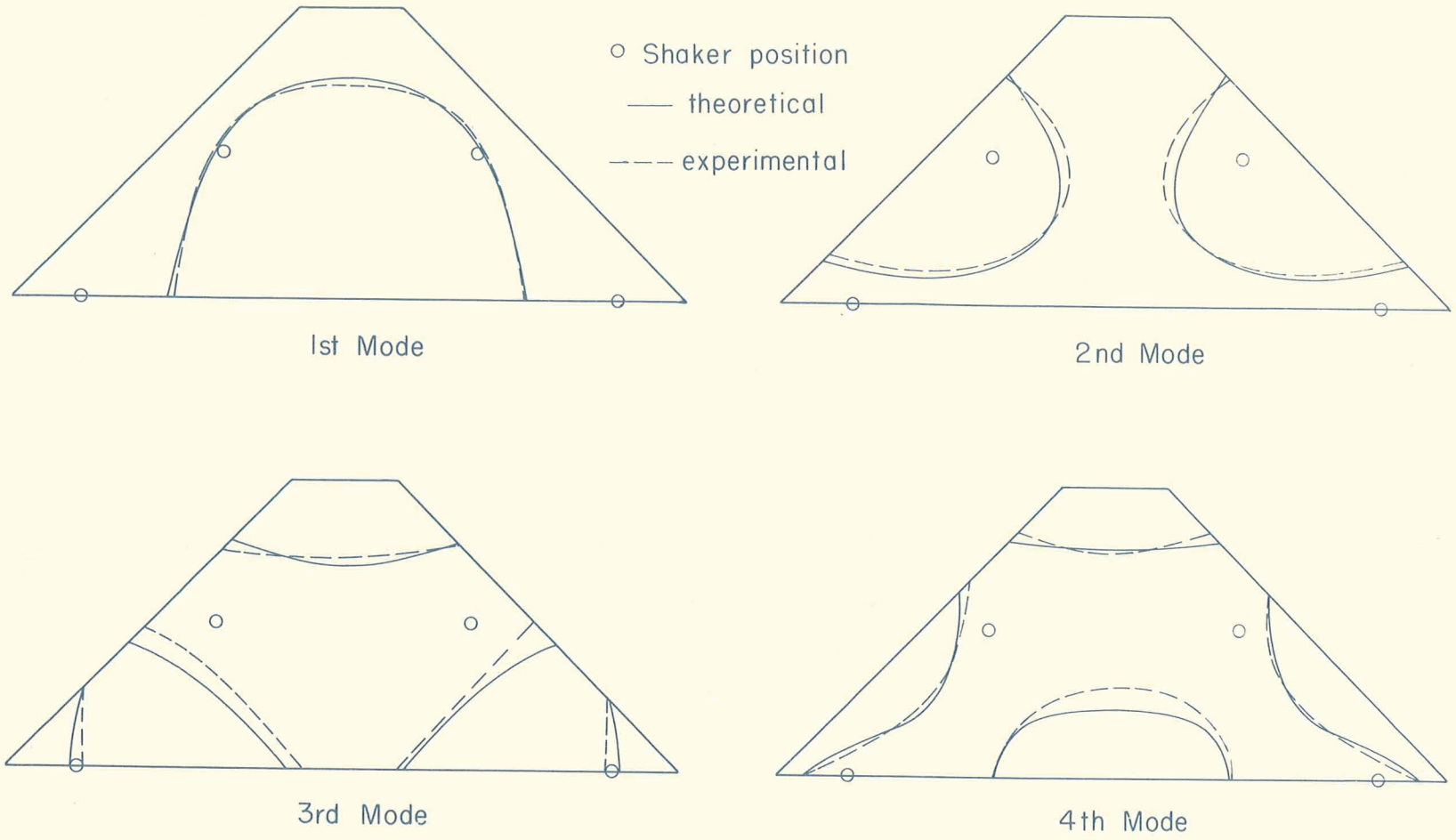

FIGURE 6

SYMMETRIC MODES FOR BUILT-UP DELTA WING SPECIMEN

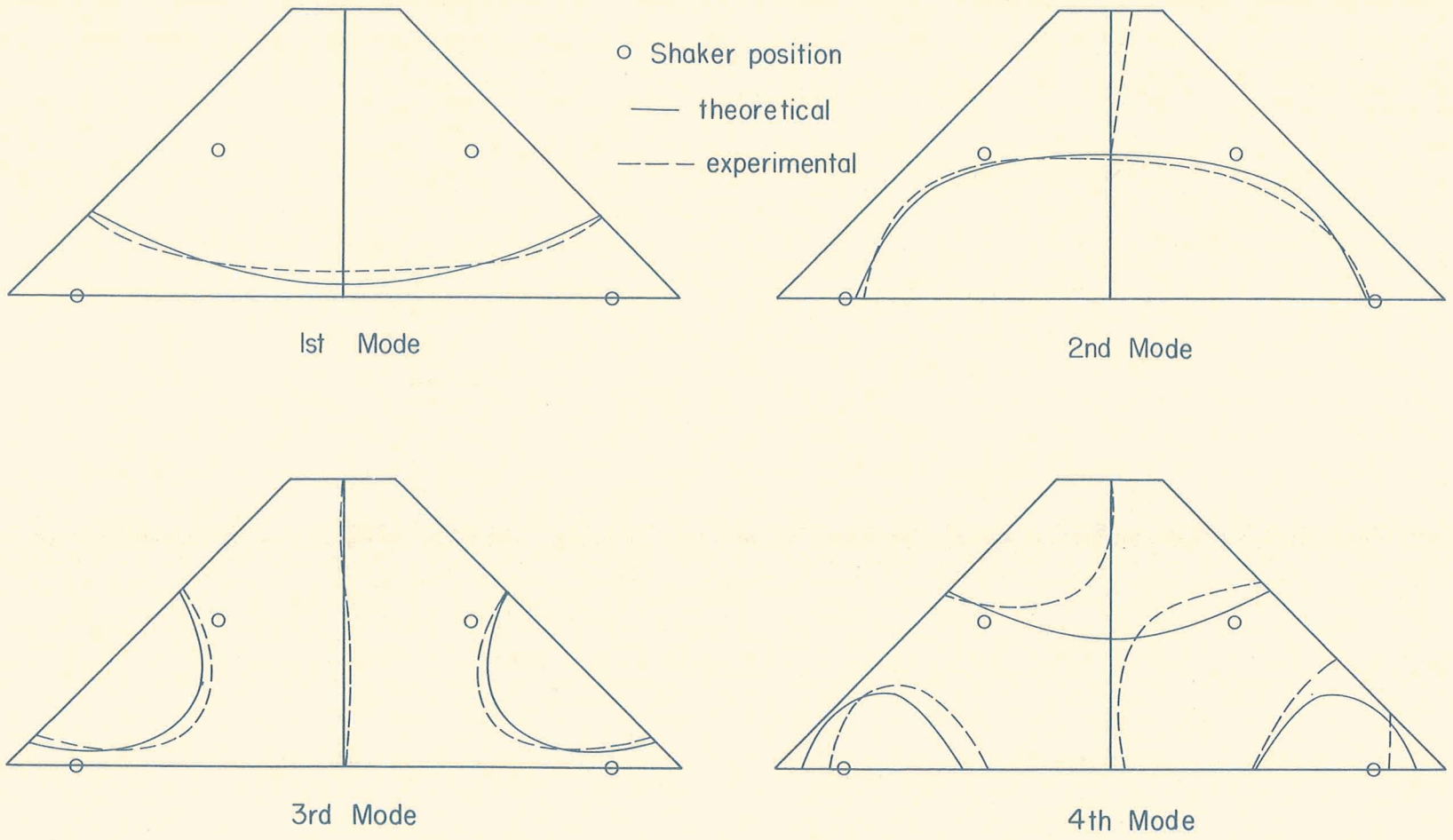

FIGURE 7

ANTISYMMETRIC MODES FOR BUILT-UP DELTA WING SPECIMEN

CHAPTER VI

DISCUSSION OF RESULTS

The theoretical frequencies obtained for the free-free vibration of the built-up wing specimen do not compare very well with the experimental frequencies. However, one thing that should be noticed in the frequency comparison is that the theoretical frequencies are always higher than the experimental frequencies. A plot of the theoretical and experimental frequencies for the first four symmetric and antisymmetric modes is shown in Figure 8. From this Figure, it is seen that the theoretical frequencies follow the experimental frequencies nicely, but that they become progressively higher as the modes increase. The reason for the theoretical frequencies being too high can be due to two things: (1) the structure of the wing, as predicted by the Stein-Sanders method, is too stiff, and (2) the mass of the wing is too low. In deriving the stiffness matrix, Stein and Sanders assumed that the spars and ribs could be represented by simple beam theory which neglects transverse shear deflections. Also, the shear lag which exists in the cover sheet is neglected. If the transverse shear deflections and the cover sheet shear lag were taken into account, the frequencies would be reduced with the frequencies of the higher modes being reduced more than the frequencies of the lower modes.

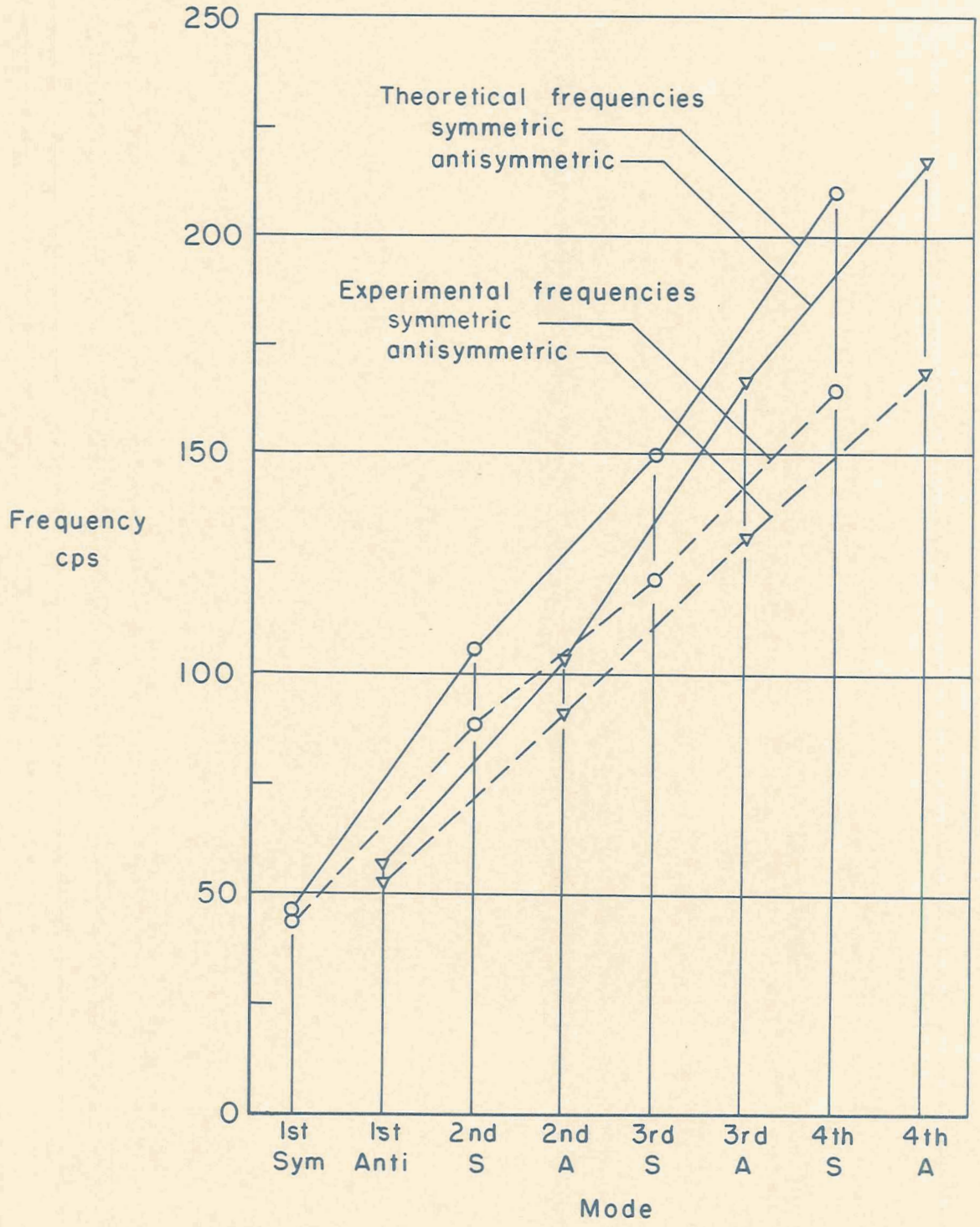

FIGURE 8

FREQUENCIES FOR BUILT-UP DELTA WING SPECIMEN

Although the wing mass used in the theoretical analysis is almost the same as the measured mass, the mass of air that surrounds the wing and is set in motion during a vibration test was neglected in the analysis. If this mass of air were added to the wing mass, then the theoretical frequencies would be reduced. Estimates show that the air mass would reduce the first frequencies by about 5 per cent, but would have a smaller effect on the higher frequencies.

Although the theoretical frequencies are much higher than the experimental frequencies, it is seen from Figures 6 and 7 that there is a remarkable agreement between the theoretical and experimental node lines.

A source of error that has not been considered yet is the power series used for the deflection shape. Since only three terms were used, the deflection of the wing was limited to a transverse displacement, twist, and parabolic chordwise curvature. It may be that three terms do not allow sufficient flexibility of the structure and more terms should be used; however, the excellent agreement between the theoretical and experimental node lines makes this possibility unlikely.

As a further source of errors we might look at the methods by which the Stein-Sanders equations were obtained. In order to keep the algebra to a minimum, trapezoidal integration was used and derivatives were replaced by

finite differences. For these procedures to be valid it is necessary that the function to be integrated or differentiated be fairly smooth. The integration involves the moment of inertia and the deflection and derivatives of the deflection; it is not expected that the integration will introduce much error. However, the numerical differentiation which involves the deflection and the derivatives of the deflection is likely to cause large errors. This is especially true of the derivatives of the Ψ_{2i} coefficients which as can be seen in Table XI do not form a very smooth curve, especially for the higher modes.

CHAPTER VII

CONCLUDING REMARKS

A comparison has been presented between the theoretical and experimental natural free-free modes and frequencies of a built-up delta wing specimen. The method of obtaining the theoretical modes and frequencies was based on the influence coefficient approach, where the influence coefficients were obtained from the Stein-Sanders method.

The results obtained from the theoretical method show that in all cases the theoretical frequencies were too high, but that the agreement between the theoretical and experimental node lines was excellent.

REFERENCES

REFERENCES

1. Levy, Samuel, "Structural Analysis and Influence Coefficients for Delta Wings," Journal of the Aeronautical Sciences, Vol. 20, No. 7, July 1953. Pp. 449-454.

2. Reissner, Eric, and Manuel Stein, "Torsion and Transverse Bending of Cantilever Plates," NACA TN 2369, 1951.

3. Schuerch, Hans U., "Zur Statik von dünnen Flugzeug-Tragflächen," Mitt. Nr. 2, Inst. für Flugzeugstatik und Flugzeugbau an der E.T.H., Leemann (Zürich), 1950.

4. Schuerch, Hans U., "Structural Analysis of Swept, Low Aspect Ratio, Multispar Aircraft Wings," Aeronautical Engineering Review, Vol. 11, No. 11, Nov. 1952. Pp. 34-41.

5. Sezawa, Katsutada, "On the Lateral Vibration of a Rectangular Plate Clamped at Four Edges," Report of the Aeronautical Research Institute, Tôkyô Imperial University, Vol. VI, 4., No. 70, April 1931.

6. Stein, Manuel, J. Edward Anderson, and John M. Hedgepeth, "Deflection and Stress Analysis of Thin Solid Wings of Arbitrary Plan Form With Particular Reference to Delta Wings," NACA Report 1131, 1953. (Supersedes NACA TN 2621)

7. Stein, Manuel, and J. L. Sanders, Jr., "A Method for Deflection Analysis of Thin Low-Aspect-Ratio Wings," NACA TN 3640, 1956.

8. Timoshenko, Stephen, Vibration Problems in Engineering. Second edition, D. Van Nostrand Co., Inc., 1937.

9. Wielandt, H., Contributions to the Mathematical Treatment of Complex Eigenvalue Problems. Part II. The Iterative Method for Not Self-Adjoint Linear Eigenvalue Problems. Reports and Translations No. 42, British M.A.P. Völkenrode, April 1, 1946. (Issued by Joint Intelligence Objectives Agency with File No. B.I.G.S. -11.)

10. Williams, D., "Recent Developments in the Structural Approach to Aerolastic Problems," Journal of the Royal Aeronautical Society, June 1954. Pp. 403-428.

11. Williams, M. L., "Theoretical and Experimental Effect of Sweep Upon the Stress and Deflection Distribution of Aircraft Wings of High Solidity. Part 6. The Plate Problem for a Cantilever Sector of Uniform Thickness," AF TR No. 5761, Part 6, Air Material Command, U. S. Air Force, Nov. 1950.

12. Young, D., "Vibration of Rectangular Plates by the Ritz Method," Journal of Applied Mechanics, Trans. A.S.M.E., Vol. 17, No. 4, 1950. Pp. 448-453.

13. Anon., Alcoa Aluminum and its Alloys. Aluminum Company of America, 1950.

APPENDIX

APPENDIX A

DERIVATION OF STIFFNESS COEFFICIENTS

In the body of this paper the method used by Stein and Sanders in reference 7 to obtain the stiffness coefficients for a low-aspect-ratio wing has only been briefly mentioned. It is the purpose of this appendix to show in greater detail how the stiffness coefficients as given by equations (11) and (13) were derived.

As the energy approach was used and the wing was considered to be composed of cover sheets, spars and stringers, and ribs, the first thing required is the strain energy expressions of these components in terms of the deflection of the neutral surface. If η represents the lateral deflection of the neutral surface, then the strain energy expressions become, for the cover sheets

$$\pi_c = \frac{1}{2} \int_0^L \int_0^{c(y)} D \left\{ \left(\frac{\partial^2 \eta}{\partial x^2} + \frac{\partial^2 \eta}{\partial y^2} \right)^2 + 2(1 - \mu) \left[\left(\frac{\partial^2 \eta}{\partial x \, \partial y} \right)^2 - \frac{\partial^2 \eta}{\partial x^2} \frac{\partial^2 \eta}{\partial y^2} \right] \right\} dx \, dy$$

where

$$D = \frac{E}{1 - \mu^2} \left(t_u z_u^2 + t_l z_l^2 \right)$$

in which the subscripts u and l refer to the upper and lower cover sheets, respectively. For the spars and stringers

$$\pi_s = \frac{1}{2}\int_0^{y_s} EI_s\left(\frac{\partial^2\eta}{\partial y^2}\right)^2 dy$$

where y_s is the end station and I_s is the moment of inertia of the sth spar or stringer. In the above energy expression slanted spars and stringers have not been considered, but their effects can easily be accounted for by a modification of this expression. For the ribs

$$\pi_r = \frac{1}{2}\int_0^{c(y_r)} EI_r\left(\frac{\partial^2\eta}{\partial x^2}\right)^2 dx$$

where $c(y_r)$ is the length and I_r is the moment of inertia of the rth rib.

The potential energy function of the transverse loads of intensity $p(x,y)$ is

$$\pi_p = -\int_0^L \int_0^{c(y)} p(x,y)\eta \, dx \, dy$$

The potential energy function which is to be minimized to obtain the equilibrium equations is

$$\pi = \pi_c + \sum_s \pi_s + \sum_r \pi_r + \pi_p$$

The method used by Stein and Sanders to minimize the above expression is first to replace the spanwise integration

by a summation in accordance with the well-known trapezoidal rule. The expression for the deflection of the neutral surface is then replaced by its equivalent power series and the resulting derivatives written in difference form. Once this has been done then the minimization process can be applied to yield a set of equations from the relation

$$\frac{\partial \pi}{\partial \Phi_{nm}} = 0$$

The resulting set of equations is expressed in matrix form by equation (11) for the symmetric case and by equation (13) for the antisymmetric case. The procedure for setting up the matrix equations has already been shown in detail for a strain energy term, for a spar or stringer, in Chapter IV when one term in the power series is used.

Since the loads enter so predominantly into the calculations it is felt worth while to consider the minimization of the potential energy function of the transverse loads for the symmetric case when three terms of the power series for the deflection are used. In this way it can be seen how the loads, moments, and second moments enter into the calculations. After the expression for the potential energy function of the transverse loads is integrated by using the trapezoidal rule and the deflection η replaced by the power series, the following expression is obtained

$$\pi_p = -\epsilon\left[\frac{1}{2}\int_0^{c(y_0)} p(x,y_0)(x^2\Phi_{20})dx + \int_0^{c(y_1)} p(x,y_1)(\Phi_{01} + x\Phi_{11} + x^2\Phi_{21})dx + \ldots + \frac{1}{2}\int_0^{c(y_N)} p(x,y_N)(\Phi_{0N} + x\Phi_{1N} + x^2\Phi_{2N})dx\right]$$

A minimization of π_p with respect to Φ_{20} yields

$$\frac{\partial\pi_p}{\partial\Phi_{20}} = -\frac{\epsilon}{2}\int_0^{c(y_0)} p(x,y_0)x^2dx$$

with respect to Φ_{01} yields

$$\frac{\partial\pi_p}{\partial\Phi_{01}} = -\epsilon\int_0^{c(y_1)} p(x,y_1)dx$$

and, with respect to Φ_{nm}

$$\frac{\partial\pi_p}{\partial\Phi_{nm}} = -\epsilon\int_0^{c(y_m)} p(x,y_m)x^{n-1}dx$$

For all the Φ's the above equation can be written in matrix form as

$$\left|\frac{\partial\pi_p}{\partial\Phi_{nm}}\right| = -\begin{vmatrix} P_{1m} \\ \hline P_{2m} \\ \hline P_{3m} \end{vmatrix}$$

where

$$P_{nm} = \epsilon p_n(y_m)$$

in which

$$p_n(y_m) = \int_0^{c(y_m)} p(x,y_m)x^{n-1}dx$$

At the end stations, one-half the value of $p_n(y_m)$ is used. This accounts for the one-half term which arises in the trapezoidal integration.